CERFACS

Centre Européen de Recherche et de Formation Avancée en Calcul Scientifique

An improved two-grid preconditioner for the solution of three-dimensional Helmholtz problems in heterogeneous media

Henri Calandra, Serge Gratton, Xavier Pinel and Xavier Vasseur

Technical Report TR/PA/12/54, revised version of TR/PA/12/2

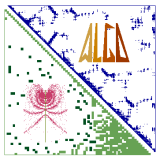

Publications of the Parallel Algorithms Team

http://www.cerfacs.fr/algor/publications/

An improved two-grid preconditioner for the solution of three-dimensional Helmholtz problems in heterogeneous media*

Henri Calandra† Serge Gratton‡ Xavier Pinel§ Xavier Vasseur¶

September 6th, 2012

Abstract

In this paper we address the solution of three-dimensional heterogeneous Helmholtz problems discretized with second-order finite difference methods with application to acoustic waveform inversion in geophysics. In this setting, the numerical simulation of wave propagation phenomena requires the approximate solution of possibly very large indefinite linear systems of equations. For that purpose, we propose and analyse an iterative two-grid method acting on the Helmholtz operator where the coarse grid problem is solved inaccurately. A cycle of a multigrid method applied to a complex shifted Laplacian operator is used as a preconditioner for the approximate solution of this coarse problem. A single cycle of the new method is then used as a variable preconditioner of a flexible Krylov subspace method. We analyse the properties of the resulting preconditioned operator by Fourier analysis. Numerical results demonstrate the effectiveness of the algorithm on three-dimensional applications. The proposed numerical method allows us to solve three-dimensional wave propagation problems even at high frequencies on a reasonable number of cores of a distributed memory computer.

Key words. Complex shifted Laplacian preconditioner; Flexible Krylov subspace methods; Helmholtz equation; Heterogeneous media; Variable preconditioning.

*Paper submitted for the special issue of Numerical Linear Algebra with Applications related to the OPTPDE ESFWaves workshop held in Würzburg, Germany, on September 26-28th 2011. Revised version.

†TOTAL, Centre Scientifique et Technique Jean Féger, avenue de Larribau F-64000 Pau, France

‡INPT-IRIT, University of Toulouse and ENSEEIHT, 2 Rue Camichel, BP 7122, F-31071 Toulouse Cedex 7, France

§CERFACS, 42 Avenue Gaspard Coriolis, F-31057 Toulouse Cedex 1, France

¶CERFACS and HiePACS project joint INRIA-CERFACS Laboratory, 42 Avenue Gaspard Coriolis, F-31057 Toulouse Cedex 1, France.

1 Introduction

The efficient simulation of wave propagation phenomena in three-dimensional heterogeneous media is of great research interest in many environmental inverse problems (e.g., monitoring of pollution in groundwater, earthquake modeling or location of hydrocarbon in fractured rocks). Such inverse problems aim at determining accurately the material properties of the subsurface by analysing the observed scattered fields after a sequence of multiple seismic shots. One of the main computational kernels of these large-scale nonlinear optimization problems is the approximate solution of a linear system issued from the discretization of a Helmholtz scalar wave equation typically written in the frequency domain. Hence the design of efficient iterative solvers for the resulting large indefinite linear systems is of major importance. This will be the main topic of the present paper.

When the medium is homogeneous (or similarly when the wavenumber is uniform), efficient multilevel solvers have been proposed in the literature. To name a few, we mention the wave-ray multigrid method [6] which exploits the structure of the error components that standard multigrid methods fail to eliminate [7] and the FETI-H nonoverlapping domain decomposition method [24], a generalization of the FETI method [25] for Helmholtz type problems, whose rate of convergence is found to be independent of the fine grid step size, the number of subdomains, and the wavenumber in many practical problems (see also, e.g., [52, Section 11.5.2]). In this paper, we rather focus on the case of three-dimensional Helmholtz problems defined in heterogeneous media for which the design of robust iterative methods that are scalable with respect to the frequency for such indefinite problems is currently an active research topic. The literature on iterative solvers for discrete Helmholtz problems is quite rich and we refer the reader to the recent survey papers [19, 23] for a taxonomy of advanced preconditioned iterative methods based on domain decomposition or multigrid.

In [2] Bayliss et al. have considered to precondition the Helmholtz operator with a different operator. A few iterations of the symmetric successive over-relaxation method were then used to approximately invert a Laplacian preconditioner. Later this work has been generalized by Laird and Giles [31], proposing a Helmholtz preconditioner with a positive sign in front of the Helmholtz term. In [18, 22] Erlangga et al. have further extended this idea: a modified Helmholtz operator with a complex wavenumber (i.e., where a complex term (hereafter named complex shift) is multiplying the square of the wavenumber) was used as a preconditioner of the Helmholtz operator. This preconditioning operator is since then referred to as a complex shifted Laplacian operator in the literature. This idea has received a lot of attention over the last few years; see among others [21, 22, 55]. Indeed with an appropriate choice of the imaginary part of the shift, standard multigrid methods can be applied successfully, i.e., the convergence of the multigrid method as a solver or as a preconditioner applied to a complex shifted Laplacian operator is mathematically found to be mesh independent at a given frequency [37]. Nevertheless, when a multigrid method applied to a shifted Laplacian operator is considered as a preconditioner for the Helmholtz operator, the convergence is found to be frequency dependent as observed in [5, 37]. This behaviour occurs independently of

the way the preconditioner is inverted (approximately or exactly). A linear increase in preconditioner applications versus the frequency is usually observed on three-dimensional problems in heterogeneous media. In practice preconditioning based on a complex shifted Laplacian operator is considered nowadays as a successful algorithm for low to medium range frequencies.

At high frequency (or equivalently at large wavenumbers), numerical results on the contrary show a steep increase in the number of outer iterations (see, e.g., [37] for a concrete application in seismic imaging). The analysis of the shifted Laplace preconditioned operator provided in [55] has indeed shown that the smallest eigenvalues of the preconditioned operator tend to zero as the wavenumber increases. Hence it becomes essential to combine this preconditioner with deflation techniques to yield an efficient numerical method as analyzed in [20, 41]. As far as we know, the resulting algorithms have not yet been applied to concrete large-scale applications on realistic three-dimensional heterogeneous problems. This is indeed a topic of current research most likely due to the complexity of the numerical method. Alternatives are required and a straightforward choice considered in, e.g., [15, 16] is to apply a multigrid cycle (with a limited number of grids in the hierarchy) to the Helmholtz operator. In [35] Pinel has proposed a two-grid cycle acting on the Helmholtz operator where the coarse grid problem is solved only inaccurately by a preconditioned Krylov subspace method. A theoretical analysis of this inexact preconditioner has been obtained by rigorous Fourier analysis [48] and numerical experiments on both homogeneous and heterogeneous problems have confirmed the theoretical developments. The convergence of the two-grid preconditioned Krylov subspace method was experimentally found to be mesh independent but still frequency dependent. This preconditioner has been successfully applied to the solution of huge Helmholtz problems on three-dimensional problems in heterogeneous media. Indeed numerical results reported in [35, Chapter 4] have demonstrated that the solution of large Helmholtz problems with billion of unknowns in seismic was tractable with such a two-grid preconditioned Krylov subspace method. Since then, this two-grid preconditioner has been applied to the solution of acoustic forward problems with multiple sources leading to multiple right-hand side problems [9] and to the solution of linear systems issued from the high-order discretization of the acoustic Helmholtz equation [8].

The numerical method presented in [35] is found to require a reduced number of preconditioner applications, each application being however computationally expensive. Indeed this cycle relies on an approximate solution of a coarse problem that is highly indefinite and ill-conditioned. Efficient algebraic one-level preconditioners to be applied on the coarse level are missing and advanced strategies should be considered to improve the convergence properties of the two-grid approach. Hence we propose to use a multigrid method applied to a shifted Laplacian operator as a preconditioner when solving the coarse problem. A single cycle of the new resulting method will be then used as a variable preconditioner for a flexible Krylov subspace method. By combining these two approaches, we expect an increased robustness of the numerical method and simultaneously a reduction of the computational cost of the two-grid cycle.

The contribution of this paper will be twofold. First, we will derive a new two-

grid preconditioner for solving Helmholtz problems in three-dimensional heterogeneous media and analyse its properties by rigorous Fourier analysis. Second, we will show the relevance of the numerical method on a challenging application in geophysics.

The paper is organized as follows. In Section 2, we introduce the acoustic Helmholtz equation written in the frequency domain and derive the discrete linear system to be solved in the forward problem. Then in Section 3 we review two different existing preconditioners based on multigrid and combine them to develop the new preconditioner. In Section 4 properties of the combined preconditioner are analysed by rigorous Fourier analysis. Furthermore we demonstrate the effectiveness of the proposed algorithm on an academic problem and on a challenging application in geophysics in Section 5. Finally we draw some conclusions in Section 6. Throughout this paper we denote by $\|.\|_2$ the Euclidean norm, $I_k \in \mathbb{C}^{k\times k}$ the identity matrix of order k and $\rho(M)$ the spectral radius of a square matrix M. Given a vector $d \in \mathbb{C}^k$ with components d_i, $D = diag(d)$ is the diagonal matrix $D \in \mathbb{C}^{k\times k}$ such that $D_{ii} = d_i, (1 \leq i \leq k)$.

2 The acoustic Helmholtz equation in the frequency domain

In this section we briefly describe the wave propagation problem associated with acoustic imaging [58] in geophysics and introduce the mathematical formulation of this problem.

2.1 Mathematical formulation

Given a three-dimensional physical domain Ω_p of parallelepiped shape, the propagation of a wavefield in a heterogeneous medium can be modeled by the Helmholtz equation written in the frequency domain [50]:

$$-\sum_{i=1}^{3}\frac{\partial^2 u}{\partial x_i^2} - \frac{(2\pi f)^2}{c^2}u \quad = \quad \delta(\mathbf{x}-\mathbf{s}), \quad \mathbf{x} = (x_1, x_2, x_3) \in \Omega_p. \tag{1}$$

In equation (1), the unknown u represents the pressure wavefield in the frequency domain, c the acoustic-wave velocity in ms^{-1}, which varies with position, and f the frequency in Hertz. The source term $\delta(\mathbf{x}-\mathbf{s})$ represents a harmonic point source located at $\mathbf{s} = (s_1, s_2, s_3) \in \Omega_p$. The wavelength λ is defined as $\lambda = c/f$ and the wavenumber as $2\pi f/c$. A popular approach - the Perfectly Matched Layer formulation (PML) [3, 4] - has been used in order to obtain a satisfactory near boundary solution, without many artificial reflections. Artificial boundary layers are then added around the physical domain to absorb outgoing waves at any incidence angle as shown in [3]. We denote by Ω_{PML} the surrounding domain created by these artificial layers. This formulation leads to the following set of coupled partial differential equations with homogeneous Dirichlet

boundary conditions imposed on Γ, the boundary of the domain:

$$-\sum_{i=1}^{3}\frac{\partial^2 u}{\partial x_i^2}-\frac{(2\pi f)^2}{c^2}u = \delta(\mathbf{x}-\mathbf{s}) \quad \text{in} \quad \Omega_p, \tag{2}$$

$$-\sum_{i=1}^{3}\frac{1}{\xi_{x_i}(x_i)}\frac{\partial}{\partial x_i}(\frac{1}{\xi_{x_i}(x_i)}\frac{\partial u}{\partial x_i})-\frac{(2\pi f)^2}{c^2}u = 0 \quad \text{in} \quad \Omega_{PML}\backslash\Gamma, \tag{3}$$

$$u = 0 \quad \text{on} \quad \Gamma, \tag{4}$$

where the one-dimensional ξ_{x_i} function represents the complex-valued damping function of the PML formulation in the i-th direction, selected as in [34]. The set of equations (2, 3, 4) defines the forward problem related to acoustic imaging in geophysics that will be considered in this paper and we note that the proposed numerical method can be applied to other application fields, where wave propagation phenomena appear as well.

2.2 Finite difference discretization

We use a standard second-order accurate seven-point finite difference discretization of the Helmholtz problem (2, 3, 4) on an uniform equidistant Cartesian grid of size $n_x \times n_y \times n_z$ (see [35, Appendix A] for a complete description of the discretization). We denote later by h the corresponding mesh grid size, Ω_h the discrete computational domain and n_{PML} the number of points in each PML layer. A fixed value of $n_{PML} = 10$ has been used hereafter. Since a stability condition has to be satisfied to correctly represent the wave propagation phenomena [11], we consider a standard second-order accurate discretization scheme with 10 points per wavelength. This implies that the mesh grid size h and the minimal wavelength in the computational domain must satisfy the following inequality [11]:

$$\frac{h}{\min_{(x_1,x_2,x_3)\in\Omega_h}\lambda(x_1,x_2,x_3)} \leq \frac{1}{10}.$$

Hereafter we have considered the following condition to determine the step size h, given a certain frequency f and an heterogeneous velocity field c:

$$h = \frac{\min_{(x_1,x_2,x_3)\in\Omega_h} c(x_1,x_2,x_3)}{10\, f}. \tag{5}$$

The discretization of the forward problem (2, 3, 4) leads to the following linear system $A_h\, x_h = b_h$, where $A_h \in \mathbb{C}^{n\times n}$ is a sparse complex matrix which is non Hermitian and non symmetric due to the PML formulation [4, 35, 46] and where $x_h, b_h \in \mathbb{C}^n$ represent the discrete frequency-domain pressure field and source, respectively. The stability condition (5) imposes to solve large systems of equations at the (usually high) frequencies of interest for the geophysicists, a task that may be too memory expensive for standard [46, 47] or advanced sparse direct methods exploiting hierarchically semi-separable structure [61, 62] on a reasonable number of cores of a parallel computer.

Consequently preconditioned Krylov subspace methods are most often considered and efficient preconditioners must be developed for such indefinite problems. Indeed, due to the indefiniteness and the ill-conditioning of the matrices A_h, these linear systems are known to be very challenging for iterative methods [23]. Efficient preconditioners must be then developed and in the last years several authors have proposed various numerical methods related to this challenging topic [5, 15, 17, 20, 21, 36, 59]. We describe next in detail a new iterative method proposed for the solution of the forward problem related to acoustic imaging.

3 Two- and multi-level preconditioned Krylov subspace method

In this section, we briefly discuss two existing preconditioning multilevel strategies for the solution of wave propagation problems presented in Section 2. Then we introduce the new two-grid preconditioner and focus on its algorithmic description.

3.1 Two-grid cycle acting on the Helmholtz operator

We first present the general framework of the two-grid preconditioner that will serve as a basis for the new method considered in this paper and introduce some notations. The fine and coarse levels denoted by h and H are associated with discrete grids Ω_h and Ω_H, respectively. Due to the application in geophysics introduced in Section 2 where structured grids are routinely used, it seems natural to consider a geometric construction of the coarse grid Ω_H. The discrete coarse grid domain Ω_H is then deduced from the discrete fine grid domain Ω_h by doubling the mesh size in each direction as classically done in vertex-centered geometric multigrid [48]. In the following, we assume that A_H represents a suitable approximation of the fine grid operator A_h on Ω_H. We also introduce $I_h^H : \mathcal{G}(\Omega_h) \rightarrow \mathcal{G}(\Omega_H)$ a restriction operator, where $\mathcal{G}(\Omega_k)$ denotes the set of grid functions defined on Ω_k. Similarly $I_H^h : \mathcal{G}(\Omega_H) \rightarrow \mathcal{G}(\Omega_h)$ will represent a given prolongation operator. More precisely, we select as a prolongation operator trilinear interpolation and as a restriction its adjoint which is often called the full weighting operator [48]. We refer the reader to [53, Section 2.9] for a complete description of these operators in three dimensions.

The two-grid cycle to be used as a preconditioner is sketched in Algorithm 1, where it is assumed that the initial approximation z_h^0 is equal to zero on Ω_h, denoted later by 0_h. As in [16, 56], polynomial smoothers based on GMRES [40] have been selected for both pre- and post-smoothing phases. Here a cycle of preconditioned GMRES(m_s) on Ω_h involves m_s matrix-vector products with A_h and $m_s\nu$ iterations of damped Jacobi. In the framework of indefinite Helmholtz problems with homogeneous velocity field, solving only approximately the coarse level problem has been analysed by rigorous Fourier analysis in [35]. Theoretical developments supported by numerical experiments have notably shown that solving approximately the coarse level problem may also lead to an efficient two-grid preconditioner. We report the reader to [35, Section 3.4] for a

Algorithm 1 Two-grid cycle applied to $A_h z_h = v_h$. $z_h = \mathcal{T}(v_h)$.

1: Polynomial pre-smoothing: Apply ϑ cycles of GMRES(m_s) to $A_h z_h = v_h$ with ν iterations of ω_h-Jacobi as a right preconditioner to obtain the approximation z_h^{ϑ}.
2: Restrict the fine level residual: $v_H = I_h^H (v_h - A_h z_h^{\vartheta})$.
3: Solve approximately the coarse problem $A_H z_H = v_H$ with initial approximation $z_H^0 = 0_H$: Apply ϑ_c cycles of GMRES(m_c) to $A_H z_H = v_H$ with ν_c iterations of ω_H-Jacobi as a right preconditioner to obtain the approximation z_H.
4: Perform the coarse level correction: $\widetilde{z_h} = z_h^{\vartheta} + I_H^h \, z_H$.
5: Polynomial post-smoothing: Apply ϑ cycles of GMRES(m_s) to $A_h z_h = v_h$ with initial approximation $\widetilde{z_h}$ and ν iterations of ω_h-Jacobi as a right preconditioner to obtain the final approximation z_h.

complete description of this analysis on three-dimensional model problems. Finally we note that the approximation at the end of the cycle z_h can be represented as $z_h = \mathcal{T}(v_h)$ where $\mathcal{T}$ is a nonlinear function due both to the use of a polynomial method based on GMRES as a smoother and to the approximate solution obtained on the coarse grid.

3.2 Multigrid cycle acting on a complex shifted Laplacian operator

A potential drawback of the two-grid cycle acting on the Helmholtz operator presented in Section 3.1 is the indefiniteness of the coarse grid problem which prevents from deriving an efficient multilevel method as recognized in [16]. In [21, 22] Erlangga et al. have exploited the pioneering idea to define a preconditioning operator based on a different partial differential equation for which a truly multilevel solution is possible. In the context of this paper, the corresponding set of equations reads as:

$$-\sum_{i=1}^{3} \frac{\partial^2 u}{\partial x_i^2} - (1+i\beta)\frac{(2\pi f)^2}{c^2} u = \delta(\mathbf{x}-\mathbf{s}) \quad \text{in} \quad \Omega_p, \tag{6}$$

$$-\sum_{i=1}^{3} \frac{1}{\xi_{x_i}(x_i)} \frac{\partial}{\partial x_i} \left(\frac{1}{\xi_{x_i}(x_i)} \frac{\partial u}{\partial x_i} \right) - (1+i\beta)\frac{(2\pi f)^2}{c^2} u = 0 \quad \text{in} \quad \Omega_{PML} \backslash \Gamma, \tag{7}$$

$$u = 0 \quad \text{on} \quad \Gamma, \tag{8}$$

where the parameter $1+i\beta \in \mathbb{C}$ is called the complex shift[1]. We introduce a sequence of l grids denoted by $\Omega_1, \cdots, \Omega_l$ (with Ω_l as the finest grid) and of appropriate operators $S_k^{(\beta)}$ $(k = 1, \cdots, l)$. Here $S_k^{(\beta)}$ is simply obtained from the second-order finite difference discretization of (6, 7, 8) on Ω_k. $S_k^{(\beta)}$ is called later the complex shifted Laplacian operator on Ω_k. In order to describe the algorithm in detail, we denote by $I_k^{k-1} : \mathcal{G}(\Omega_k) \to \mathcal{G}(\Omega_{k-1})$ a restriction operator from Ω_k to Ω_{k-1}, $I_{k-1}^k : \mathcal{G}(\Omega_{k-1}) \to \mathcal{G}(\Omega_k)$ a

[1] In [22] the authors have introduced the complex shifted Laplacian with a negative imaginary part for the shift in the case of first- or second-order radiation boundary conditions. Due to the PML formulation considered in this paper, we have used a shift with positive imaginary part to derive an efficient preconditioner as explained in [35, Section 3.3.2].

prolongation operator from Ω_{k-1} to Ω_k and C the cycling strategy (which can be of V, F or W type). The complex shifted multigrid algorithm considered in this paper is then sketched in Algorithm 2.

Algorithm 2 Multigrid cycle (with a hierarchy of l grids) applied to $S_l^{(\beta)} y_l = w_l$. $y_l = \mathcal{M}_{l,C}(w_l)$.

1: Pre-smoothing: Apply ν_β iterations of ω_l-Jacobi to $S_l^{(\beta)} y_l = w_l$ to obtain the approximation $y_l^{\nu_\beta}$.
2: Restrict the fine level residual: $w_{l-1} = I_l^{l-1}(w_l - S_l^{(\beta)} y_l^{\nu_\beta})$.
3: Solve approximately the coarse problem $S_{l-1}^{(\beta)} y_{l-1} = w_{l-1}$ with initial approximation $y_{l-1}^0 = 0_{l-1}$: Apply recursively γ cycles of multigrid to $S_{l-1}^{(\beta)} y_{l-1} = w_{l-1}$ to obtain the approximation y_{l-1}. On the coarsest level ($l = 1$) apply ϑ_β cycles of GMRES(m_β) preconditioned by ν_β iterations of ω_1-Jacobi to $S_1^{(\beta)} y_1 = w_1$ as an approximate solver.
4: Perform the coarse level correction: $\widetilde{y}_l = y_l^{\nu_\beta} + I_{l-1}^l y_{l-1}$.
5: Post-smoothing: Apply ν_β iterations of ω_l-Jacobi to $S_l^{(\beta)} y_l = w_l$ with initial approximation $\widetilde{y}_l$ to obtain the final approximation y_l.

In Algorithm 2, the γ parameter controls the type of cycling strategy of the multigrid hierarchy, see, e.g., [48]. Trilinear interpolation and full-weighting are used as prolongation and restriction operators, respectively. An approximate solution on the coarsest level is considered as in the two-grid approach proposed in Section 3.1. We note that the approximation at the end of the cycle y_l can be represented as $y_l = \mathcal{M}_{l,C}(w_l)$ where $\mathcal{M}_{l,C}$ is a nonlinear function since a Krylov subspace method (namely preconditioned GMRES(m_β)) is used as an approximate solver on the coarsest grid Ω_1.

The multigrid cycle of Algorithm 2 is based on a Jacobi smoother as promoted in [21] and slightly differs from the original algorithm proposed in [21]. Indeed Erlangga et al. in [21] have used the matrix-dependent interpolation operator of [64], a Galerkin coarse grid approximation to deduce the discrete coarse operators and an exact solution on the coarsest grid. For three-dimensional applications, Erlangga [19] and Riyanti et al. [37] have proposed a multigrid method with a two-dimensional semi-coarsening strategy combined with line-wise damped Jacobi smoothing in the third direction. A cycle of multigrid acting on this complex shifted Laplacian operator is then considered as a preconditioner for the Helmholtz operator and the theoretical properties of this preconditioner have been investigated in [55]. Since its introduction, this preconditioning technique based on a different partial differential equation has been extensively used, see, e.g., [5, 17, 37, 59] for applications in three dimensions.

3.3 Combined cycle

One of the main difficulties related to the two-grid preconditioner presented in Section 3.1 is that the coarse linear system is strongly indefinite at large wavenumbers due to

the stability condition (5). Consequently, even a loose approximate solution is found to be computationally expensive to obtain with standard preconditioned Krylov subspace solvers. To circumvent this difficulty, we introduce a multigrid cycle acting on a complex shifted Laplacian operator as a preconditioner for the coarse grid system $A_H z_H = v_H$ defined on Ω_H. The complex shifted Laplacian operator is simply obtained by direct coarse grid discretization of equations (6,7,8) on Ω_H. The new cycle can be seen as a combination of two cycles defined on two different hierarchies. First, a two-grid cycle using Ω_h and Ω_H only as fine and coarse levels respectively is applied to the Helmholtz operator. Second, a sequence of grids Ω_k ($k = 1, \cdots, l$) with the finest grid Ω_l defined as $\Omega_l := \Omega_H$ is introduced. On this second hierarchy a multigrid cycle applied to a complex shifted Laplacian operator $S_H^{(\beta)} := S_l^{(\beta)}$ is then used as a preconditioner when solving the coarse level system $A_H z_H = v_H$ of the two-grid cycle. The new combined cycle is sketched in Algorithm 3.

Algorithm 3 Combined cycle applied to $A_h z_h = v_h$. $z_h = \mathcal{T}_{l,C}(v_h)$.

1: Polynomial pre-smoothing: Apply ϑ cycles of GMRES(m_s) to $A_h z_h = v_h$ with ν iterations of ω_h-Jacobi as a right preconditioner to obtain the approximation z_h^{ϑ}.
2: Restrict the fine level residual: $v_H = I_h^H (v_h - A_h z_h^{\vartheta})$.
3: Solve approximately the coarse problem $A_H z_H = v_H$ with initial approximation $z_H^0 = 0_H$: Apply ϑ_c cycles of FGMRES(m_c) to $A_H z_H = v_H$ preconditioned by a cycle of multigrid applied to $S_l^{(\beta)} y_l = w_l$ on $\Omega_l \equiv \Omega_H$ yielding $y_l = \mathcal{M}_{l,C}(w_l)$ to obtain the approximation z_H.
4: Perform the coarse level correction: $\widetilde{z_h} = z_h^{\vartheta} + I_H^h z_H$.
5: Polynomial post-smoothing: Apply ϑ cycles of GMRES(m_s) to $A_h z_h = v_h$ with initial approximation $\widetilde{z_h}$ and ν iterations of ω_h-Jacobi as a right preconditioner to obtain the final approximation z_h.

The notation $\mathcal{T}_{l,C}$ uses subscripts related to the cycle applied to the shifted Laplacian operator (i.e. number of grids l of the second hierarchy and cycling strategy C (which can be of V, F or W type), respectively). The combined cycle then involves discretization of operators on $l + 1$ grids in total. Hence later in the numerical experiments we will compare $\mathcal{T}_{l,C}$ with $\mathcal{M}_{l+1,C}$. Figure 1 shows a possible configuration with a three-grid cycle applied to the shifted Laplacian operator. The combined cycle is related to the recursively defined K-cycle introduced in [33]. Nevertheless we note that the combined cycle relies on a preconditioning operator on the coarse level that is different from the original operator. The approximation at the end of the cycle z_h can be represented as $z_h = \mathcal{T}_{l,C}(v_h)$ where $\mathcal{T}_{l,C}$ is a nonlinear function obtained as a combination of functions introduced in Sections 3.1 and 3.2, respectively. Consequently, this cycle leads to a variable nonlinear preconditioner which must be combined with an outer *flexible* Krylov subspace method [43, 44] and [57, Chapter 10]. We have selected an outer Krylov subspace method of minimum residual type, namely flexible GMRES (FGMRES(m)) [38]. This choice allows us to characterize effectively the quality of the preconditioner even on realistic problems at a cheap cost as discussed later in Section 5.3.

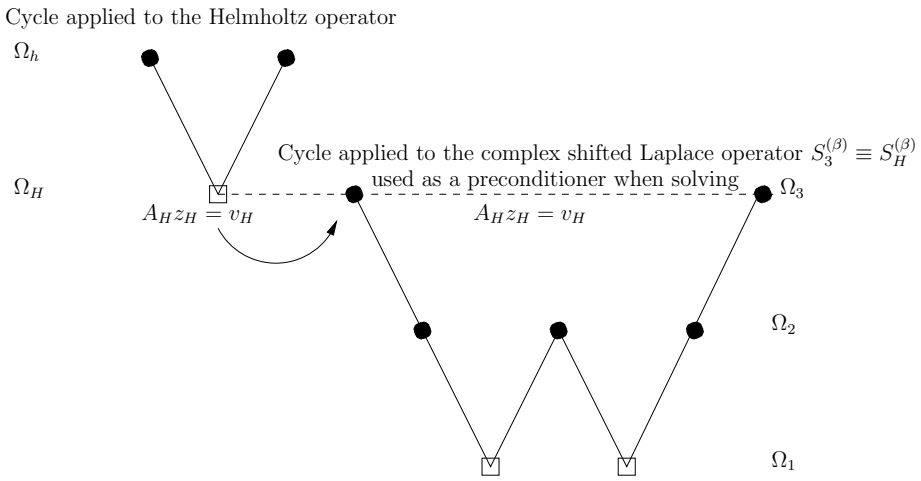

Figure 1: Combined cycle applied to $A_h z_h = v_h$ sketched in Algorithm 3. Case of $\mathcal{T}_{3,F}$. The two-grid cycle is applied to the Helmholtz operator (left part), whereas the three-grid cycle to be used as a preconditioner when solving the coarse grid problem $A_H z_H = v_H$ is shown on the right part. This second multigrid cycle acts on the shifted Laplacian operator with β as a shift parameter.

4 Fourier analysis of multigrid preconditioners

In this section, we provide a two-grid rigorous Fourier analysis to select appropriate relaxation parameters in the smoother and to understand the convergence properties of the two-grid methods used as a preconditioner introduced in Section 3. For this analysis only, we consider a two-grid method based on a Jacobi smoother, standard coarsening, full-weighting, trilinear interpolation and exact solution on the coarse grid, applied to a model problem of Helmholtz type. We refer the reader to [48, 51] for the theoretical foundations of rigorous Fourier analysis.

4.1 Rigorous Fourier analysis

Notation Throughout Section 4, we consider the complex shifted Laplace equation with a uniform wavenumber given by $k = 2\pi f/c$ on the unit cube $\Omega = [0,1]^3$ and homogeneous Dirichlet boundary conditions on the boundary of the domain:

$$-\Delta u - \kappa_\beta^2 u = g \quad \text{in} \quad \Omega, \tag{9}$$

$$u = 0 \quad \text{on} \quad \partial\Omega, \tag{10}$$

with κ_β defined as $\kappa_\beta^2 = (1+\beta i)k^2$, where β denotes a real parameter lying in $[0,1]$. A classical tool in multigrid theory to deduce some information about the two-grid convergence rate is based on a rigorous Fourier analysis (RFA) [53, Section 3.3.4]. To perform this analysis, we introduce some additional notations. First, we discretize the

model problem (9, 10) on an uniform mesh of step size $\varkappa = 1/n_\varkappa$. We denote by $L_\varkappa^{(\beta)}$ the corresponding discrete operator on the considered fine grid $\Omega_\varkappa = G_\varkappa \cap [0,1]^3$ where $G_\varkappa$ is the infinite grid and by $D_\varkappa^{(\beta)}$ the matrix corresponding to the diagonal part of $L_\varkappa^{(\beta)}$. The discrete eigenfunctions of $L_\varkappa^{(\beta)}$:

$$\varphi_\varkappa^{l_1,l_2,l_3}(x,y,z) = \sin(l_1\pi x)\,\sin(l_2\pi y)\,\sin(l_3\pi z) \text{ with } l_1,l_2,l_3 = 1,...,n_\varkappa - 1 \text{ and } (x,y,z) \in \Omega_\varkappa,$$

generate the space of all fine grid functions, $F(\Omega_\varkappa)$, and are orthogonal with respect to the discrete inner product on $\Omega_\varkappa$:

$$(v_\varkappa, w_\varkappa) := \varkappa^3 \sum_{(x,y,z)\in\Omega_\varkappa} v_\varkappa(x,y,z) w_\varkappa(x,y,z) \quad \text{with } v_\varkappa, w_\varkappa \in F(\Omega_\varkappa).$$

The space of all fine grid real-valued functions $F(\Omega_\varkappa)$ can be divided into a direct sum of (at most) eight-dimensional subspaces - called the $2\varkappa$-harmonics [53, Equation (3.4.1)] - :

$$\begin{aligned} E_\varkappa^{l_1,l_2,l_3} \;=\; & span[\varphi_\varkappa^{l_1,l_2,l_3}, -\varphi_\varkappa^{n_\varkappa-l_1,n_\varkappa-l_2,n_\varkappa-l_3}, -\varphi_\varkappa^{n_\varkappa-l_1,l_2,l_3}, \varphi_\varkappa^{l_1,n_\varkappa-l_2,n_\varkappa-l_3}, \\ & -\varphi_\varkappa^{l_1,n_\varkappa-l_2,l_3}, \varphi_\varkappa^{n_\varkappa-l_1,l_2,n_\varkappa-l_3}, -\varphi_\varkappa^{l_1,l_2,n_\varkappa-l_3}, \varphi_\varkappa^{n_\varkappa-l_1,n_\varkappa-l_2,l_3}], \\ & \text{for } l_1,l_2,l_3 = 1,\cdots,n_\varkappa/2. \end{aligned}$$

The dimension of $E_\varkappa^{l_1,l_2,l_3}$, denoted by $\eta_\varkappa^{l_1,l_2,l_3}$, is eight, four, two and one if zero, one, two or three of the indices l_1,l_2,l_3 is equal to $n_\varkappa/2$, respectively. Similarly as on the fine grid $\Omega_\varkappa$, we introduce the discrete eigenfunctions of the coarse grid operator $L_{2\varkappa}^{(\beta)}$ on the space of all coarse grid functions $F(\Omega_{2\varkappa})$ with $\Omega_{2\varkappa} = G_{2\varkappa} \cap [0,1]^3$:

$$\varphi_{2\varkappa}^{l_1,l_2,l_3}(x,y,z) = \sin(l_1\pi x)\,\sin(l_2\pi y)\,\sin(l_3\pi z), \text{ with } l_1,l_2,l_3 = 1,...,\frac{n_\varkappa}{2} - 1 \text{ and } (x,y,z) \in \Omega_{2\varkappa}.$$

$E_{2\varkappa}^{l_1,l_2,l_3}$ is then defined as $span[\varphi_{2\varkappa}^{l_1,l_2,l_3}]$ since the eigenfunctions of $L_{2\varkappa}$ coincide up to their sign on $\Omega_{2\varkappa}$ for $l_1,l_2,l_3 = 1,\cdots,n_\varkappa/2$ [53]. We denote later by ℓ the multi-index $\ell = (l_1,l_2,l_3)$, by $\mathcal{L}_\varkappa = \{\ell \;|1 \le \max(l_1,l_2,l_3) < n_\varkappa/2\}$ and by $\mathcal{H}_\varkappa = \{\ell \;|n_\varkappa/2 \le \max(l_1,l_2,l_3) < n_\varkappa\}$ the sets of multi-indices corresponding to the low-frequency and high-frequency harmonics, respectively. We also define the set $\mathcal{L}_\varkappa^= = \{\ell \,|1 \le \max(l_1,l_2,l_3) \le n_\varkappa/2\}$. Later in this section, the Fourier representation of a given discrete operator $M_\varkappa$ is denoted by $\widehat{M}_\varkappa$ and the restriction of $\widehat{M}_\varkappa$ to $E_\varkappa^\ell$ with $\ell \in \mathcal{L}_\varkappa$ is noted $\widehat{M}_\varkappa(\ell) = \widehat{M}_{\varkappa|E_\varkappa^\ell}$ in short. The Fourier representation of the discrete Helmholtz operator $L_\varkappa^{(\beta)}$ and the Jacobi iteration matrix $J_\varkappa^{(\beta)}$ are denoted $\widehat{L}_\varkappa^{(\beta)}$ and $\widehat{J}_\varkappa^{(\beta)}$, respectively. To write the Fourier representation of these operators in a compact form, we also introduce the ξ_i parameters such that $\xi_i = \sin^2\left(\dfrac{l_i\pi\varkappa}{2}\right)$ for $i = 1,2,3$. Finally we denote by $\varkappa = h$ the finest mesh grid size considered, n_h the corresponding number of points per direction and $k_\varkappa$ the wavenumber on the grid with mesh size $\varkappa$.

4.2 Smoothing analysis

The multigrid method acting on a complex shifted Laplacian operator presented in Algorithm 2 is based on a Jacobi smoother as used in [21] in two dimensions. Indeed in [21] it has been numerically shown that this method enjoys good smoothing properties on all the grids of the hierarchy when the relaxation parameters $\omega_\varkappa$ are well chosen. In Proposition 1, we give the Fourier representation of the Jacobi iteration matrix $J_\varkappa^{(\beta)}$ applied to the complex shifted Laplacian matrix $L_\varkappa^{(\beta)}$. Then we derive related smoothing factors and by numerical experiments we deduce appropriate damping parameters to obtain good smoothing properties in three dimensions.

Proposition 1. *The harmonic spaces $E_\varkappa^\ell$ for $\ell \in \mathcal{L}_\varkappa^=$ are invariant under the Jacobi iteration matrix $J_\varkappa^{(\beta)} = I_\varkappa - \omega_\varkappa (D_\varkappa^{(\beta)})^{-1} L_\varkappa^{(\beta)}$ ($J_\varkappa^{(\beta)} : E_\varkappa^\ell \longrightarrow E_\varkappa^\ell$, for $\ell \in \mathcal{L}_\varkappa^=$). The operator $J_\varkappa^{(\beta)}$ is orthogonally equivalent to a block diagonal matrix of (at most) 8×8 blocks defined as:*

$$\widehat{J}_\varkappa^{(\beta)}(\ell) \;=\; I_{\eta_\varkappa^\ell} - \left(\frac{\omega_\varkappa \varkappa^2}{6 - (\kappa_\beta \varkappa)^2} \right) \widehat{L}_\varkappa^{(\beta)}(\ell), \quad \ell \in \mathcal{L}_\varkappa^=, \tag{11}$$

where $\widehat{L}_\varkappa^{(\beta)}$ denotes the representation of the complex shifted Laplacian operator $L_\varkappa^{(\beta)}$ with respect to the space $E_\varkappa^\ell$ and $\eta_\varkappa^\ell$ the dimension of $E_\varkappa^\ell$, respectively. With notation introduced in Section 4.1, if $\ell \in \mathcal{L}_\varkappa$, the representation of $\widehat{L}_\varkappa^{(\beta)}$ with respect to $E_\varkappa^\ell$ is a diagonal matrix defined as:

$$\widehat{L}_\varkappa^{(\beta)}(\ell) \;=\; diag \left(\frac{4}{\varkappa^2} \begin{pmatrix} (\xi_1 + \xi_2 + \xi_3) \\ (3 - \xi_1 - \xi_2 - \xi_3) \\ (1 - \xi_1 + \xi_2 + \xi_3) \\ (2 + \xi_1 - \xi_2 - \xi_3) \\ (1 + \xi_1 - \xi_2 + \xi_3) \\ (2 - \xi_1 + \xi_2 - \xi_3) \\ (1 + \xi_1 + \xi_2 - \xi_3) \\ (2 - \xi_1 - \xi_2 + \xi_3) \end{pmatrix} \begin{matrix} -\kappa_\beta^2 \\ -\kappa_\beta^2 \\ -\kappa_\beta^2 \\ -\kappa_\beta^2 \\ -\kappa_\beta^2 \\ -\kappa_\beta^2 \\ -\kappa_\beta^2 \\ -\kappa_\beta^2 \end{matrix} \right), \quad \ell \in \mathcal{L}_\varkappa. \tag{12}$$

If one of the indices of ℓ equals $n_\varkappa/2$, $\widehat{L}_\varkappa^{(\beta)}(\ell)$ degenerates to a diagonal matrix of dimension $\eta_\varkappa^\ell$. Its entries then correspond to the first $\eta_\varkappa^\ell$ entries of the matrix given on the right-hand side of relation (12).

Proof. Obviously, since the eigenfunctions spanning $E_\varkappa^\ell$ are eigenfunctions of $L_\varkappa^{(\beta)}$, the harmonic spaces $E_\varkappa^\ell$ ($\ell \in \mathcal{L}_\varkappa$) are invariant under $L_\varkappa^{(\beta)}$ and hence invariant under $J_\varkappa^{(\beta)}$. The representation of $L_\varkappa^{(\beta)}$ with respect to the harmonic space $E_\varkappa^\ell$ is obtained by writing the eigenvalues of the basis functions of $E_\varkappa^\ell$ in terms of ξ_i, a straightforward calculation that only involves trigonometric identities. □

The representation of the Jacobi iteration matrix in the Fourier space obtained in Proposition 1 allows us to easily investigate its smoothing properties, i.e., to compute

the smoothing factor μ versus various parameters (β, mesh grid size $\varkappa$, wavenumber $k_\varkappa$ and relaxation parameter $\omega_\varkappa$, respectively). With ν denoting the number of relaxation sweeps, the smoothing factor $\mu(\beta, \varkappa, k_\varkappa, \omega_\varkappa)$ is defined as follows [63]:

$$\mu(\beta, \varkappa, k_\varkappa, \omega_\varkappa) \quad = \quad \max_{\ell \in \mathcal{L}_\varkappa^=} |(\rho(\widehat{Q}_\varkappa(\ell)\ (\widehat{J}_\varkappa^{(\beta)}(\ell))^\nu)^{1/\nu}|, \tag{13}$$

where $\widehat{Q}_\varkappa$ is the matrix representation of a projection operator that annihilates the low-frequency error components and leaves the high-frequency components unchanged [48], e.g., $\widehat{Q}_\varkappa(\ell) = diag((0,1,1,1,1,1,1,1)^T)$ for $\ell \in \mathcal{L}_\varkappa$. In addition if we assume that $\kappa_\beta \varkappa$ (or similarly $k_\varkappa \varkappa$) is a given constant (which is the case in practice due to the stability condition to be satisfied) it is then possible to deduce the supremum $\mu^\star(\beta, \varkappa, k_\varkappa, \omega_\varkappa)$ of the smoothing factor over $\varkappa$ as:

$$\mu^\star(\beta, \varkappa, k_\varkappa, , \omega_\varkappa) \quad = \quad \max \left\{ |1 - \omega_\varkappa \frac{2 - \kappa_\beta^2 \varkappa^2}{6 - \kappa_\beta^2 \varkappa^2}|, |1 - \omega_\varkappa \frac{12 - \kappa_\beta^2 \varkappa^2}{6 - \kappa_\beta^2 \varkappa^2}| \right\}, \tag{14}$$

or similarly:

$$\mu^\star(\beta, \varkappa, k_\varkappa, \omega_\varkappa) = \max \left\{ |1 - \omega_\varkappa + \frac{4\omega_\varkappa}{6 - (1+i\beta) k_\varkappa^2 \varkappa^2}|, |1 - \omega_\varkappa - \frac{6\omega_\varkappa}{6 - (1+i\beta) k_\varkappa^2 \varkappa^2}| \right\}. \tag{15}$$

For a fixed value of $k_\varkappa \varkappa$ this formula can then give guidance in choosing the optimal relaxation parameters and in understanding how the optimal value of the relaxation parameter $\omega_\varkappa^\star$ depends on $k_\varkappa \varkappa$ and on β, respectively. Indeed a simple calculation gives the real-valued optimal relaxation parameter as:

$$\omega_\varkappa^\star = 1 - \frac{1}{7 - k_\varkappa^2 \varkappa^2}.$$

We notice that the optimal value of the relaxation parameter does not depend on the shift parameter β and note that we recover the optimal relaxation parameter and the supremum of the smoothing factor of the Jacobi method for the Poisson equation in three dimensions when $k_\varkappa$ is set to zero [53, Section 2.9.2].

Fourier results We select two relaxation sweeps ($\nu = 2$) in the Jacobi method and compute the smoothing factor $\mu(\beta, \varkappa, k_\varkappa, \omega_\varkappa)$ for different values of the shift parameter β, $\omega_\varkappa$ on four consecutive grids in the multigrid hierarchy ($\varkappa = h, \varkappa = 2h, \varkappa = 4h, \varkappa = 8h$); see Figure 2. The selected wavenumbers satisfy the relation[2] $k_\varkappa = \frac{n_h}{n_\varkappa} \frac{\pi}{5h}$ (or similarly $k_\varkappa = \frac{\varkappa}{h} \frac{\pi}{5h}$) and we consider the case of $n_h = 512$ on the finest grid.

From Figure 2 we observe a similar behaviour as was obtained in the two-dimensional case in [16, 21]. Smoothing difficulties do occur neither on the fine grid nor on the coarsest

[2] This corresponds to the stability condition (5) on the finest grid and to practical situations of interest on the other coarse grids of the hierarchy.

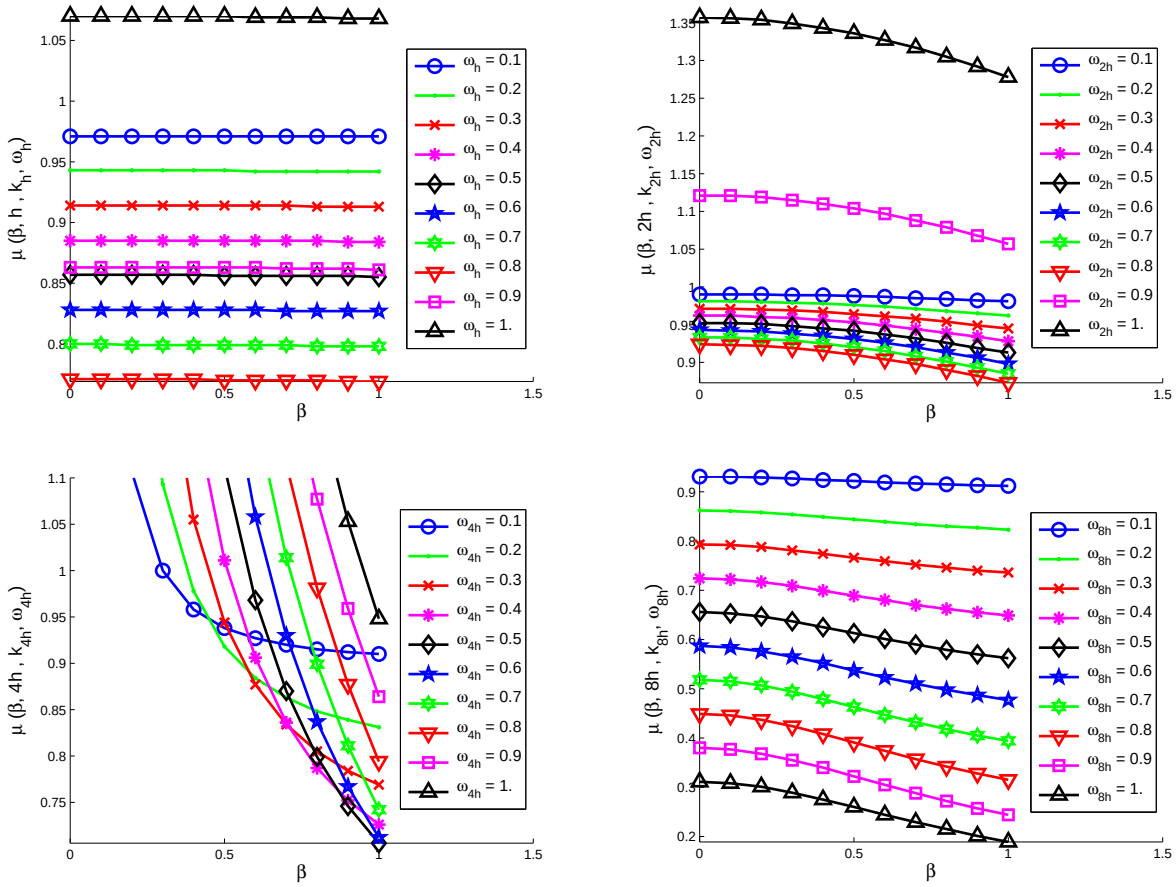

Figure 2: Smoothing factors $\mu(\beta, \varkappa, k_\varkappa, \omega_\varkappa)$ of the Jacobi method (see equation (13)) versus β and $\omega_\varkappa$ considering 2 relaxation sweeps ($\nu = 2$) on four different grids ($\varkappa = h$, $\varkappa = 2h$, $\varkappa = 4h$, $\varkappa = 8h$) on the model problem (9, 10). Case of $\varkappa = h$ (top left), $\varkappa = 2h$ (top right), $\varkappa = 4h$ (bottom left) and $\varkappa = 8h$ (bottom right). The wavenumber $k_\varkappa$ is defined as $k_\varkappa = \dfrac{n_h}{n_\varkappa}\dfrac{\pi}{5h}$ with $n_h = 512$.

grid of the multigrid hierarchy but on intermediate grids only. Indeed, when $\varkappa = 4h$ (bottom left part of Figure 2), smoothing factors less than one cannot be obtained unless using a complex shifted Laplace operator with $\beta \geq 0.4$. Consequently - and in agreement with the discussion provided in [21] in the two-dimensional case - we have decided to fix the shift parameter to $\beta = 0.5$. According to Figure 2, this choice leads us to consider the following relaxation parameters: $\omega_h = 0.8$, $\omega_{2h} = 0.8$, $\omega_{4h} = 0.2$, $\omega_{8h} = 1$ or in short:

$$(\omega_h, \omega_{2h}, \omega_{4h}, \omega_{8h}) = (0.8, 0.8, 0.2, 1). \tag{16}$$

These relaxation parameters will be selected in Section 5 and we note that that they are close to the optimal values based on (15) given in Table 1.

Table 1: Optimal smoothing factors $\mu^\star(\beta, \varkappa, k_\varkappa, \omega_\varkappa)$ and optimal relaxation parameters $\omega^\star_\varkappa$ versus $\varkappa$ on the model problem (9, 10) for two values of the shift parameter β. The wavenumber $k_\varkappa$ is defined as $k_\varkappa = \dfrac{n_h}{n_\varkappa}\dfrac{\pi}{5h}$ with h designing the stepsize of the finest grid ($n_h = 512$).

	$\beta = 0$		$\beta = 0.5$	
$\varkappa$	$\mu^\star(\beta, k_\varkappa\varkappa, \omega^\star_\varkappa)$	$\omega^\star_\varkappa$	$\mu^\star(\beta, k_\varkappa\varkappa, \omega^\star_\varkappa)$	$\omega^\star_\varkappa$
h	0.757	0.848	0.756	0.848
$2h$	0.922	0.815	0.908	0.815
$4h$	> 1		0.918	0.193
$8h$	0.274	1.055	0.231	1.055

Finally it has been shown that reasonably good smoothing factors for the Jacobi smoother can be obtained on all the grid hierarchy for the complex shifted Laplacian operator in three dimensions; seel also [12] where a local Fourier analysis of the damped Jacobi method is performed on the complex shifted Laplacian in one and two dimensions. With the selected relaxation parameters we now investigate the spectrum of preconditioned Helmholtz matrices.

4.3 Fourier analysis of preconditioned Helmholtz operator

As shown in [63], the rigorous Fourier analysis can also provide the spectrum of a two-grid preconditioned operator inexpensively. This feature is notably quite helpful when analysing the convergence of a given preconditioned Krylov subspace method, here restarted GMRES. Next, we will perform this analysis not only on the fine level ($\varkappa = h$) to characterize the quality of the two-grid preconditioners but also on the second level ($\varkappa = 2h$) where preconditioners proposed in Algorithms 2 and 3 will be investigated. We first briefly describe how to deduce the representation of these preconditioned operators in the Fourier space.

4.3.1 Iteration matrix of a two-grid cycle

Assumptions on the components of the cycle In this paragraph, we assume that both the fine grid operator and the smoother leave the spaces $E_\varkappa^\ell$ invariant for $\ell \in \mathcal{L}_\varkappa^=$. As shown in Proposition 1, $L_\varkappa^{(\beta)}$ and the corresponding Jacobi iteration matrix $J_\varkappa^{(\beta)}$ do satisfy this invariance property. Furthermore we assume that the transfer operators $I_\varkappa^{2\varkappa}$, $I_{2\varkappa}^\varkappa$ satisfy the following relations:

$$I_\varkappa^{2\varkappa} : E_\varkappa^\ell \rightarrow span[\varphi_{2\varkappa}^\ell], \quad I_{2\varkappa}^\varkappa : span[\varphi_{2\varkappa}^\ell] \rightarrow E_\varkappa^\ell, \quad \text{for } \ell \in \mathcal{L}_\varkappa. \tag{17}$$

and that the coarse discretization operator leaves the subspace $span[\varphi_{2\varkappa}^\ell]$ invariant for $\ell \in \mathcal{L}_\varkappa$. We note that the discrete coarse Helmholtz matrix $L_{2\varkappa}^{(\beta)}$ satisfies this last property and that the trilinear interpolation and its adjoint also satisfy relation (17) [53].

Proposition 2. *If the previous assumptions are satisfied, the iteration matrix of the two-grid cycle ($M_\varkappa^{(\beta)} : E_\varkappa^\ell \longrightarrow E_\varkappa^\ell$, for $\ell \in \mathcal{L}_\varkappa^=$) leaves the spaces of $2\varkappa$-harmonics $E_\varkappa^\ell$ with an arbitrary $\ell \in \mathcal{L}_\varkappa^=$ invariant. The Fourier representation of the two-grid iteration matrix $M_\varkappa^{(\beta)}$ is as a block-diagonal matrix of (at most) 8×8 blocks defined as:*

$$\widehat{M}_\varkappa^{(\beta)}(\ell) \quad = \quad (\widehat{J}_\varkappa^{(\beta)}(\ell))^\nu \widehat{K}_{\varkappa,2\varkappa}^{(\beta)}(\ell)(\widehat{J}_\varkappa^{(\beta)}(\ell))^\nu \quad \textit{for} \quad \ell \in \mathcal{L}_\varkappa^=, \tag{18}$$

with $\widehat{K}_{\varkappa,2\varkappa}^{(\beta)}(\ell) = I_8 - [c\, d^T]/\Lambda_{2\varkappa}^{(\beta)}$ *if* $\ell \in \mathcal{L}_\varkappa$, *where* $\Lambda_{2\varkappa}^{(\beta)} = \dfrac{4}{\varkappa^2}((1-\xi_1)\xi_1 + (1-\xi_2)\xi_2 + (1-\xi_3)\xi_3) - \kappa_\beta^2$ *and* $c \in \mathbb{R}^8$, $d \in \mathbb{C}^8$, *are defined as follows:*

$$\begin{cases} c_1 = (1-\xi_1)(1-\xi_2)(1-\xi_3),\ c_2 = \xi_1\xi_2\xi_3,\ c_3 = \xi_1(1-\xi_2)(1-\xi_3),\ c_4 = (1-\xi_1)\xi_2\xi_3, \\ c_5 = (1-\xi_1)\xi_2(1-\xi_3),\ c_6 = \xi_1(1-\xi_2)\xi_3,\ c_7 = (1-\xi_1)(1-\xi_2)\xi_3,\ c_8 = \xi_1\xi_2(1-\xi_3), \\ d = \widehat{L}_\varkappa^{(\beta)}(\ell)\ c, \ \textit{where } \widehat{L}_\varkappa^{(\beta)}(\ell) \textit{ is defined in equation (12).} \end{cases}$$

If one of the indices of ℓ is equal to $n_\varkappa/2$, $\widehat{K}_{\varkappa,2\varkappa}^{(\beta)}(\ell)$ is reduced to the identity matrix of dimension $\eta_\varkappa^\ell$.

Proof. Under the assumptions given above, it is straightforward to prove that the iteration matrix of the two-grid cycle leaves $E_\varkappa^\ell$ for $\ell \in \mathcal{L}_\varkappa^=$ invariant. We obtain formula (18) by just combining the Fourier representation of each of its components. The complete details of these trigonometric calculations can be found in [35, Section 3.3.1]. □

4.3.2 Fourier representation of preconditioned Helmholtz operator

In this paragraph, we consider the solution of the following linear system $L_\varkappa^{(\sigma_L)} y_\varkappa = w_\varkappa$ with a given Krylov subspace method. The corresponding matrix $L_\varkappa^{(\sigma_L)}$ is a possibly complex shifted Laplacian matrix with $\kappa_{\sigma_L}^2 = (1 + i\sigma_L)k_\varkappa^2 \in \mathbb{C}$, $k_\varkappa = \dfrac{n_h}{n_\varkappa}\dfrac{\pi}{5h}$ where $\varkappa$ is the mesh grid size and σ_L denotes a shift parameter lying in $[0, 1]$. The preconditioning matrix can be a two-grid iteration matrix $M_\varkappa^{(\sigma_p)}$ or a Jacobi iteration matrix $J_\varkappa^{(\sigma_p)}$,

both applied to a possibly complex shifted Laplacian operator $L_\varkappa^{(\sigma_p)}$ with $\kappa_{\sigma_p}^2 = (1 + i\sigma_p)k_\varkappa^2$, where σ_p denotes a shift parameter lying in $[0, 1]$. Each preconditioning step requires an approximate solution of the linear system $L_\varkappa^{(\sigma_p)} z_\varkappa = v_\varkappa$. If one cycle of a geometric two-grid method is used to approximate the inverse of $L_\varkappa^{(\sigma_p)}$, we denote by $\mho_\varkappa^{-1}(\sigma_p)$ this approximation. Similarly, if ν relaxation sweeps of a Jacobi method is used to approximate the inverse of $L_\varkappa^{(\sigma_p)}$, we denote by $\Upsilon_\varkappa^{-1}(\sigma_p)$ this approximation. The convergence of the Krylov subspace method with right preconditioning is partly related to the spectra of the matrices $L_\varkappa^{(\sigma_L)}\,\mho_\varkappa^{-1}(\sigma_p)$ or $L_\varkappa^{(\sigma_L)}\Upsilon_\varkappa^{-1}(\sigma_p)$. As shown in [63], the iteration matrices of both preconditioning phases correspond to:

$$M_\varkappa^{(\sigma_p)} = (I_\varkappa - \mho_\varkappa^{-1}(\sigma_p)\, L_\varkappa^{(\sigma_p)}) \qquad \text{or} \qquad \mho_\varkappa^{-1}(\sigma_p)\, L_\varkappa^{(\sigma_p)} = I_\varkappa - M_\varkappa^{(\sigma_p)}, \tag{19}$$

$$J_\varkappa^{(\sigma_p)^\nu} = (I_\varkappa - \Upsilon_\varkappa^{-1}(\sigma_p)\, L_\varkappa^{(\sigma_p)}) \qquad \text{or} \qquad \Upsilon_\varkappa^{-1}(\sigma_p)\, L_\varkappa^{(\sigma_p)} = I_\varkappa - J_\varkappa^{(\sigma_p)^\nu}. \tag{20}$$

From (19) and (20), the following relations can be easily deduced :

$$L_\varkappa^{(\sigma_L)}\,\mho_\varkappa^{-1}(\sigma_p) = L_\varkappa^{(\sigma_L)}\,(I_\varkappa - M_\varkappa^{(\sigma_p)})\,(L_\varkappa^{(\sigma_p)})^{-1}\,, \tag{21}$$

$$L_\varkappa^{(\sigma_L)}\,\Upsilon_\varkappa^{-1}(\sigma_p) = L_\varkappa^{(\sigma_L)}\,(I_\varkappa - J_\varkappa^{(\sigma_p)^\nu})\,(L_\varkappa^{(\sigma_p)})^{-1}\,. \tag{22}$$

Remark Since all operators in Equation (21) are block diagonal in the Fourier space (see Propositions 1 and 2, respectively), the spectrum of $L_\varkappa^{(\sigma_L)}\,\mho_\varkappa^{-1}(\sigma_p)$ is obtained by solving eigenvalue problems of small dimension only (8 at most). This is inexpensive. We also remark that the Fourier representation of $L_\varkappa^{(\sigma_L)}\,\Upsilon_\varkappa^{-1}(\sigma_p)$ is a diagonal matrix (see Proposition 1), its spectrum is then obtained straightforwardly.

4.3.3 Fourier results

Fine level $\varkappa = h$ - Figure 3 We first analyse the spectrum of $L_h^{(\sigma_L)}\,\mho_h^{-1}(\sigma_p)$ for $\sigma_L = 0$ (i.e. the Helmholtz operator) with two different preconditioners. We will consider the case of a preconditioner based on a two-grid method acting either on the Helmholtz operator ($\sigma_p = 0$) or on a complex shifted Laplacian operator ($\sigma_p = 0.5$). The corresponding spectra of $L_h^{(0)}\,\mho_h^{-1}(0)$ and $L_h^{(0)}\,\mho_h^{-1}(0.5)$ are shown in Figure 3.

Using the two-grid method on the Helmholtz operator leads to a spectrum with a cluster around $(1, 0)$ in the complex plane with relatively a few isolated eigenvalues with both positive and negative real parts (left part of Figure 3). When the two-grid method is applied to the complex shifted Laplacian matrix, the spectrum shown on the right part of Figure 3 is lying in the positive real part of the complex plane only with relatively few eigenvalues close to zero (less than 0.1% of the spectrum is located inside the disk of radius 0.1 centered at the origin). Moreover, it has to be noticed that the shapes of these spectra are similar to those obtained in two dimensions; see Figure 1 in [14] for the Helmholtz matrix and Figure 7 in [21] (up to a symmetry with respect to the x-axis) for the complex shifted Laplacian matrix, respectively. Both spectra relatively look in favor of the convergence of a Krylov subspace method as will be confirmed by numerical experiments on a homogeneous Helmholtz problem in Section 5.2.

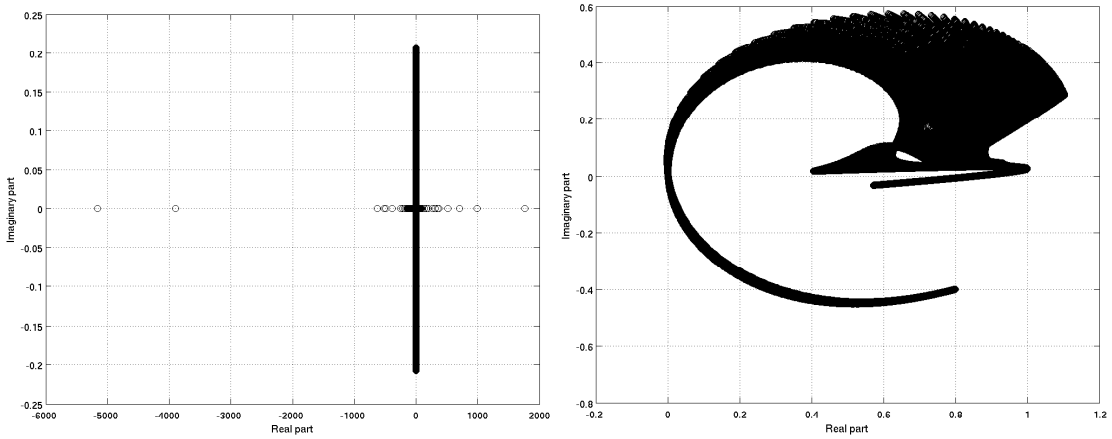

Figure 3: Spectra of $L_h^{(0)}\,\mho_h^{-1}(\sigma_p)$ for two different two-grid preconditioners ($\sigma_p = 0$, $\omega_h = 0.8$, $\nu = 2$) (left part) and ($\sigma_p = 0.5$, $\omega_h = 0.8$, $\nu = 2$) (right part), with $h = \dfrac{1}{256}$ for a wavenumber such as $k_h = \pi/(5h)$. Note the different scales used in both figures.

Coarse level $\varkappa = 2h$ - Figure 4 We now study the preconditioner properties on the coarse level in a two-grid method acting on the Helmholtz problem. More precisely we consider two different preconditioners to solve the indefinite coarse problem approximately. First, two iterations ($\nu = 2$) of damped Jacobi with $\omega_{2h} = 0.8$ are used as a preconditioner of the coarse Helmholtz matrix (see step 3 of Algorithm 1). The spectrum of $L_{2h}^{(0)}\,\Upsilon_{2h}^{-1}(0)$ is shown on the left part of Figure 4. Second, a complex shifted multigrid method is used to solve approximately the coarse Helmholtz problem (see step 3 of Algorithm 3). The spectrum of the preconditioned coarse Helmholtz matrix $L_{2h}^{(0)}\,\mho_{2h}^{-1}(0.5)$ is shown on the right part of Figure 4.

If we compare the two plots related to the complex shifted multigrid preconditioner (right parts of Figures 3 and 4, respectively), we remark that both spectra have a similar curved shape. Most of the eigenvalues have a real part located between 0. and 1.2, whereas only a few outliers have a negative real part close to zero. A similar behaviour in terms of convergence is then expected on both fine and coarse levels when such a preconditioner is used. On the opposite, the Jacobi coarse preconditioner acts quite differently. No cluster appears in the spectrum shown on the left part of Figure 4 and even worse the real part of the eigenvalues is located between 0 and 2 million with a few outliers having a negative real part close to zero. This spread of eigenvalues in the spectrum may strongly penalize the convergence of GMRES on the coarse level ($\varkappa = 2h$). Consequently, according to both spectra shown in Figure 4, the preconditioner based on a cycle of multigrid applied to a complex shifted Laplacian operator seems to be a more appropriate choice to solve the coarse Helmholtz problem approximately.

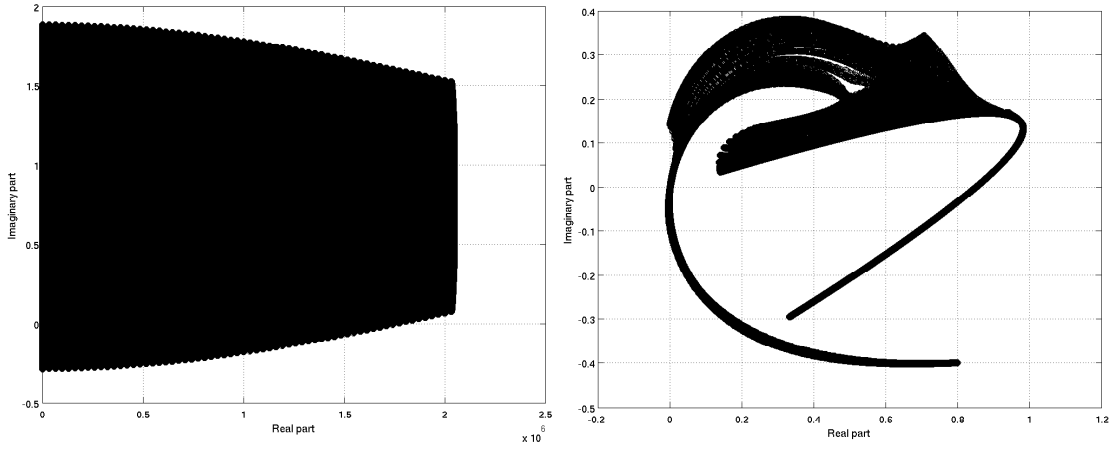

Figure 4: Spectrum of $L_{2h}^{(0)}\,\Upsilon_{2h}^{-1}(\sigma_p)$ ($\sigma_p = 0$, $\omega_r = 0.8$, $\nu = 2$) (left part) and of $L_{2h}^{(0)}\,\mho_{2h}^{-1}(\sigma_p)$ ($\sigma_p = 0.5$, $\omega_{2h} = 0.8$, $\nu = 2$) (right part), with $h = \dfrac{1}{256}$ for a wavenumber k_{2h} such that $k_{2h} = 2\pi/(5h)$. Note the different scales used in both figures.

Coarse level $\varkappa = 4h$ - Figure 5 We conclude this analysis by studying the properties of the Jacobi preconditioner on the coarsest level ($\varkappa = 4h$) in a complex shifted multigrid cycle (see step 3 of Algorithm 2). The spectrum of $L_{4h}^{(\sigma_L)}\,\Upsilon_{4h}^{-1}(\sigma_p)$ is shown in Figure 5 for $\sigma_L = \sigma_p = 0.5$ with $\nu = 2$ relaxation sweeps of damped Jacobi ($\omega_{4h} = 0.2$) as a preconditioner. This spectrum looks in favor of the convergence of GMRES. Indeed the preconditioned matrix $L_{4h}^{(0.5)}\,\Upsilon_{4h}^{-1}(0.5)$ is actually a positive definite complex matrix and satisfies a sufficient condition to ensure the convergence of GMRES [39, Theorem 6.30].

4.4 Rigorous Fourier analysis for operators with variable coefficients

In this subsection only we consider the complex shifted Laplace equation now with smoothly variable coefficients on the unit cube $\Omega = [0,1]^3$ and homogeneous Dirichlet boundary conditions on the boundary of the domain:

$$-\sum_{i=1}^{3} \frac{1}{\xi_{x_i}(x_i)} \frac{\partial}{\partial x_i}\Big(\frac{1}{\xi_{x_i}(x_i)} \frac{\partial u}{\partial x_i}\Big) - \kappa_\beta^2 u = g \quad \text{in} \quad \Omega, \tag{23}$$

$$u = 0 \quad \text{on} \quad \partial\Omega. \tag{24}$$

This model problem aims at representing the partial differential equation to be solved when using the PML formulation. We denote by $L_\varkappa^{(\beta)}(x)$ and $D_\varkappa^{(\beta)}(x)$ the discretized operator with variable coefficients on the considered fine grid $\Omega_\varkappa$ and its diagonal part respectively. A direct application of rigorous Fourier analysis is not possible for partial differential equations with variable coefficients [28, 53]. The smoothing factor indeed becomes x-dependent. However the analysis can be applied to the locally frozen operator

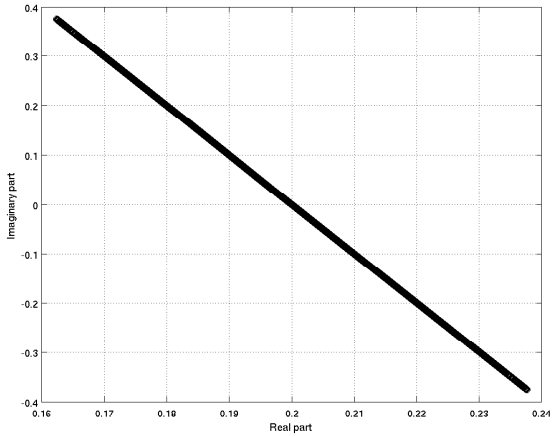

Figure 5: Spectrum of $L_{4h}^{(\sigma_L)}\,\Upsilon_{4h}^{-1}(\sigma_p)$, with $\sigma_L = \sigma_p = 0.5$, $\omega_{4h} = 0.2$, $\nu = 2$, $h = \dfrac{1}{256}$ on a 64^3 grid with $k_{4h} = 4\pi/(5h)$.

$L_{\varkappa}^{(\beta)}(x_f)$ at a fixed grid point $x_f \in \Omega$ of coordinates $(x_{f_1}, x_{f_2}, x_{f_3})$: it reduces to perform the rigorous Fourier analysis on the operator with frozen coefficients. To perform such analysis we now assume that the finite difference stencil notation of the discretized operator $L_{\varkappa}^{(\beta)}(x_f)$ can be written as:

$$L_{\varkappa,(0)}^{(\beta)}(x_f) = \frac{1}{\varkappa^2}\begin{bmatrix} & -\chi_2 & \\ -\chi_1 & 2(\chi_1+\chi_2+\chi_3) - (\kappa_\beta \varkappa)^2 & -\chi_1 \\ & -\chi_2 & \end{bmatrix}$$

$$L_{\varkappa,(-1)}^{(\beta)}(x_f) = \frac{1}{\varkappa^2}\begin{bmatrix} -\chi_3 \end{bmatrix}, \quad L_{\varkappa,(1)}^{(\beta)}(x_f) = \frac{1}{\varkappa^2}\begin{bmatrix} -\chi_3 \end{bmatrix}$$

with $\chi_i \in \mathbb{C}$ $(i = 1, 2, 3)$ defined as $1/(\xi_{x_i}^2(x_{f_i}))$. First we extend Proposition 1 to the case of partial differential equations with variable coefficients.

4.4.1 Smoothing factor

Proposition 3. *At a given point $x_f \in \Omega_\varkappa$ the harmonic spaces $E_\varkappa^\ell$ for $\ell \in \mathcal{L}_\varkappa^=$ are invariant under the Jacobi iteration matrix $J_\varkappa^{(\beta)}(x_f) = I_\varkappa - \omega_\varkappa (D_\varkappa^{(\beta)}(x_f))^{-1} L_\varkappa^{(\beta)}(x_f)$ $(J_\varkappa^{(\beta)}(x_f) : E_\varkappa^\ell \longrightarrow E_\varkappa^\ell$, for $\ell \in \mathcal{L}_\varkappa^=)$. The operator $J_\varkappa^{(\beta)}(x_f)$ is orthogonally equivalent to a block diagonal matrix of (at most) 8×8 blocks defined as:*

$$\widehat{J}_\varkappa^{(\beta)}(\ell, x_f) \;=\; I_{\eta_\varkappa^\ell} - \left(\frac{\omega_\varkappa \varkappa^2}{2(\chi_1+\chi_2+\chi_3) - (\kappa_\beta \varkappa)^2}\right) \widehat{L}_\varkappa^{(\beta)}(\ell, x_f), \ell \in \mathcal{L}_\varkappa^=, \qquad (25)$$

where $\widehat{L}_\varkappa^{(\beta)}(x_f)$ denotes the representation of the complex shifted Laplacian operator $L_\varkappa^{(\beta)}(x_f)$ with respect to the space $E_\varkappa^\ell$ at point x_f and $\eta_\varkappa^\ell$ the dimension of $E_\varkappa^\ell$, re-

spectively. With notation introduced in Section 4.1, if $\ell \in \mathcal{L}_\varkappa$, the representation of $\widehat{L}_\varkappa^{(\beta)}(x_f)$ with respect to $E_\varkappa^\ell$ is a diagonal matrix defined as:

$$\widehat{L}_\varkappa^{(\beta)}(\ell, x_f) \;=\; diag\left(\frac{4}{\varkappa^2}\begin{pmatrix} (\chi_1\xi_1 + \chi_2\xi_2 + \chi_3\xi_3) \\ (\chi_1(1-\xi_1) + \chi_2(1-\xi_2) + \chi_3(1-\xi_3)) \\ (\chi_1(1-\xi_1) + \chi_2\xi_2 + \chi_3\xi_3) \\ (\chi_1\xi_1 + \chi_2(1-\xi_2) + \chi_3(1-\xi_3)) \\ (\chi_1\xi_1 + \chi_2(1-\xi_2) + \chi_3\xi_3) \\ (\chi_1(1-\xi_1) + \chi_2\xi_2 + \chi_3(1-\xi_3)) \\ (\chi_1\xi_1 + \chi_2\xi_2 + \chi_3(1-\xi_3)) \\ (\chi_1(1-\xi_1) + \chi_2(1-\xi_2) + \chi_3\xi_3) \end{pmatrix} \begin{matrix} -\kappa_\beta^2 \\ -\kappa_\beta^2 \\ -\kappa_\beta^2 \\ -\kappa_\beta^2 \\ -\kappa_\beta^2 \\ -\kappa_\beta^2 \\ -\kappa_\beta^2 \\ -\kappa_\beta^2 \end{matrix}\right) \quad (26)$$

If one of the indices of ℓ equals $n_\varkappa/2$, $\widehat{L}_\varkappa^{(\beta)}(\ell, x_f)$ degenerates to a diagonal matrix of dimension $\eta_\varkappa^\ell$. Its entries then correspond to the first $\eta_\varkappa^\ell$ entries of the matrix given on the right-hand side of relation (26).

Proof. This can be obtained by using trigonometric identities as in Proposition 1. □

The worst-case smoothing factor $\mu_{wc}(\beta, \varkappa, k_\varkappa, \omega_\varkappa)$ is then defined as:

$$\begin{aligned} \mu_{wc}(\beta, \varkappa, k_\varkappa, \omega_\varkappa) &= \max_{x_f \in \Omega} \mu(\beta, \varkappa, k_\varkappa, \omega_\varkappa, x_f), \\ &= \max_{x_f \in \Omega} \max_{\ell \in \mathcal{L}_\varkappa^=} |(\rho(\widehat{Q}_\varkappa(\ell)\ (\widehat{J}_\varkappa^{(\beta)}(\ell, x_f))^\nu)^{1/\nu}|. \end{aligned}$$

As an illustration, Figure 6 shows the smoothing factors at a selected point x_f chosen in the PML layer such as $1/\chi_j = (1 + i\cos(3\pi/8))^2, (j = 1, 2, 3)$ (with a PML function selected as in [34]) for different values of β on four different grids ($\varkappa = h$, $\varkappa = 2h$, $\varkappa = 4h$, $\varkappa = 8h$, respectively) with a wavenumber defined as $k_\varkappa = \dfrac{n_h}{n_\varkappa}\dfrac{\pi}{5h}$ with $n_h = 512$. For such a choice of the χ_j coefficients we note that smoothing factors less than one can be obtained on the intermediate coarse grid $\varkappa = 4h$ whatever β. When β is set to 0.5, Table 2 reveals that reasonable worst-case values of the smoothing factors can be obtained on the different grids as in Section 4.2. On the other hand, for the considered combination of $\omega_\varkappa$, $k_\varkappa$ and $\varkappa$ it is possible to obtain worst-case values of the smoothing factor greater than one when β is equal to 0; this justifies the use of a Krylov acceleration procedure as a smoother as recommended in [16].

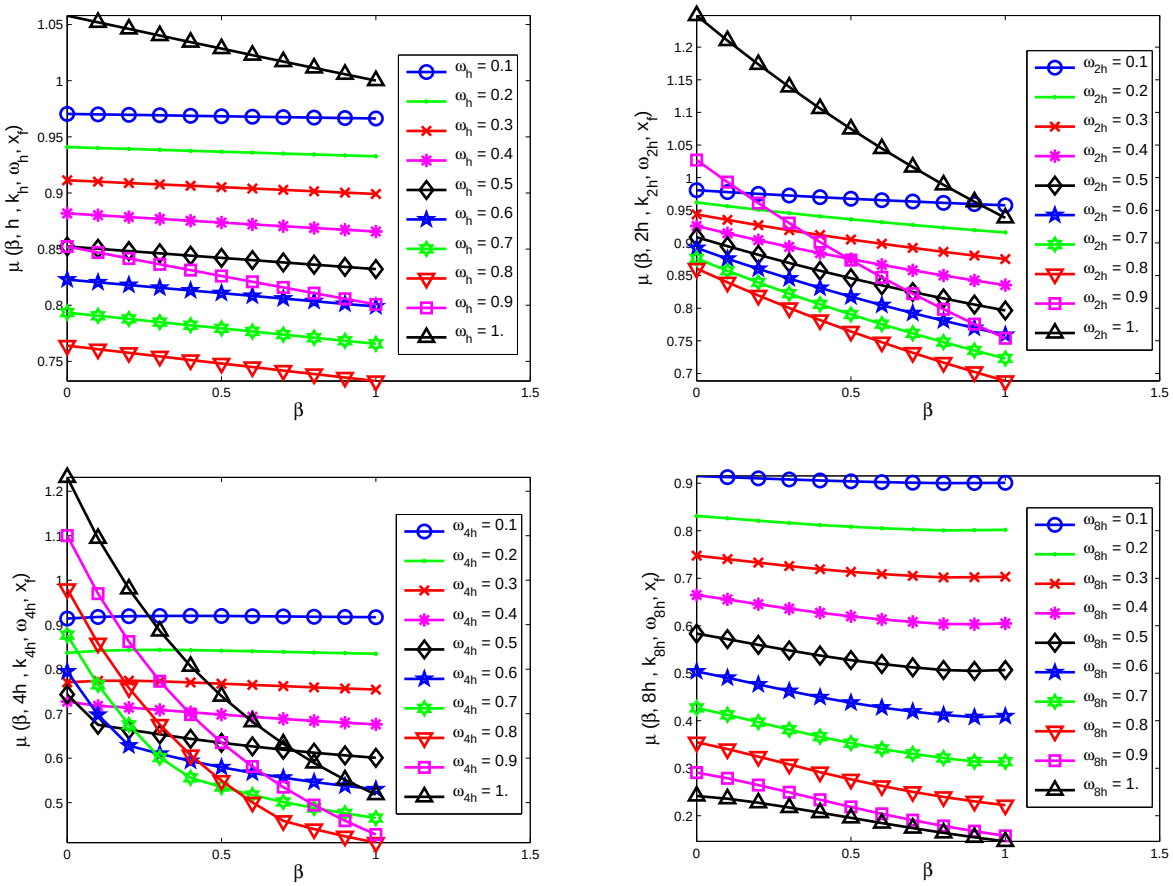

Figure 6: Smoothing factors $\mu(\beta, \varkappa, k_\varkappa, \omega_\varkappa, x_f)$ of the Jacobi method versus β and $\omega_\varkappa$ considering 2 relaxation sweeps ($\nu = 2$) on four different grids ($\varkappa = h$, $\varkappa = 2h$, $\varkappa = 4h$, $\varkappa = 8h$) on the model problem (23, 24). Case of $\varkappa = h$ (top left), $\varkappa = 2h$ (top right), $\varkappa = 4h$ (bottom left) and $\varkappa = 8h$ (bottom right). The wavenumber $k_\varkappa$ is defined as $k_\varkappa = \dfrac{n_h}{n_\varkappa}\dfrac{\pi}{5h}$ with $n_h = 512$. Case of $1/\chi_j = (1 + i\cos(3\pi/8))^2, (j = 1, 2, 3)$.

Table 2: Computed worst-case smoothing factors $\mu_{wc}(\beta, \varkappa, k_\varkappa, \omega_\varkappa)$ for the model problem (23, 24) for two values of β versus $\varkappa$. The wavenumber $k_\varkappa$ is defined as $k_\varkappa = \frac{n_h}{n_\varkappa}\frac{\pi}{5h}$ with $n_h = 512$.

	$\beta = 0$		$\beta = 0.5$	
$\varkappa$	$\mu_{wc}(\beta, \varkappa, k_\varkappa, \omega_\varkappa)$	$\omega_\varkappa$	$\mu_{wc}(\beta, \varkappa, k_\varkappa, \omega_\varkappa)$	$\omega_\varkappa$
h	0.791	0.8	0.770	0.8
$2h$	> 1	0.8	0.914	0.8
$4h$	> 1	0.2	0.918	0.2
$8h$	0.310	1	0.260	1

4.5 Conclusions

To conclude, we have selected with the rigorous Fourier analysis appropriate relaxation parameters in the Jacobi method that lead to acceptable smoothing factors on all the grids of a complex shifted multigrid method in three dimensions (Figure 3). As a new result, we have shown the suitability of the complex shifted multigrid preconditioner on the coarse level of a combined two-grid method (left part of Figure 4). Finally we have also demonstrated the good preconditioning properties of a Jacobi preconditioner on the coarsest level of a complex shifted multigrid (Figure 5). Although rigorous Fourier analysis corresponds to a simplified analysis, numerical experiments detailed in Section 5 will support these conclusions.

5 Numerical experiments on three-dimensional problems

We investigate the performance of the various preconditioners presented in Section 3 combined with Flexible GMRES(m) for the solution of the acoustic Helmholtz problem (2, 3, 4) on an homogeneous problem and on a realistic heterogeneous velocity model.

5.1 Settings

In the two-grid cycle of Algorithm 1, we consider as a smoother the case of one cycle of GMRES(2) preconditioned by two iterations of damped Jacobi ($\vartheta = 1$, $m_s = 2$ and $\nu = 2$), a restarting parameter equal to $m_c = 10$ for the preconditioned GMRES method used on the coarse level and a maximal number of coarse cycles equal to $\vartheta_c = 10$. In the complex shifted multigrid cycle of Algorithm 2, we use a shift parameter equal to $\beta = 0.5$ and two iterations of damped Jacobi as a smoother ($\nu_\beta = 2$). On the coarsest level we consider as an approximate solver one cycle of GMRES(10) preconditioned by two iterations of damped Jacobi ($\vartheta_\beta = 1$, $m_\beta = 10$ and $\nu_\beta = 2$). The previous parameters have been also used in Algorithm 3, exception made for ϑ_c set to 2. Finally the relaxation coefficients considered in the Jacobi method have been determined by rigorous Fourier analysis and are given by relation (16).

We consider a value of the restarting parameter of the outer Krylov subspace method equal to $m = 5$ as in [9, 35] (see the first remark given in Section 5.3 for further comments). The unit source is located at $(s_1, s_2, s_3) = (h\ n_{x_1}/2, h\ n_{x_2}/2, h\ (n_{PML}+1))$ where, e.g., n_{x_1} denotes the number of points in the first direction. A zero initial guess x_h^0 is chosen and the iterative method is stopped when the Euclidean norm of the residual normalized by the Euclidean norm of the right-hand side satisfies the following relation:

$$\frac{||b_h - A_h x_h||_2}{||b_h||_2} \leq 10^{-5}. \tag{27}$$

The numerical results have been obtained on Babel, a IBM Blue Gene/P computer located at IDRIS (each node of Babel is equipped with 4 PowerPC 450 cores at 850 Mhz) using a Fortran 90 implementation with MPI [27] in complex single precision arithmetic (see [53, Chapter 6] for the practical aspects related to the parallelization of geometric multigrid). Physical memory on a given node (4 cores) of Babel is limited to 2 GB. This code was compiled by the IBM compiler suite with the best optimization options and linked with the vendor BLAS and LAPACK subroutines.

5.2 Homogeneous velocity field

We consider the case of an homogeneous velocity field in a reference domain $[0, 1]^3$ as a first benchmark problem. The step size of the Cartesian mesh of type n_h^3 is given by $h = 1/n_h$ and a uniform wavenumber k is imposed such that $kh = \pi/5$ as stated in relation (5). Consequently large wavenumbers are obtained when the step size h is small. Table 3 collects the number of preconditioner applications (Prec), computational times (T) and maximal requested memory (M) for the various preconditioners investigated in Section 3: a two-grid preconditioner ($\mathcal{T}$), two four-grid complex shifted preconditioners ($\mathcal{M}_{4,V}$ and $\mathcal{M}_{4,F}$) and three variants of two-grid cycles with complex shifted two-grid cycle ($\mathcal{T}_{2,V}$) or three-grid cycles ($\mathcal{T}_{3,V}$ and $\mathcal{T}_{3,F}$) as a coarse preconditioner, respectively. Finally the number of cores (# Cores) is selected such that the dimension of the local problem on the finest grid is fixed for a given strategy in these numerical experiments.

The number of preconditioner applications (Prec) is found to grow almost linearly with the wavenumber, whatever the preconditioning strategies. This behaviour has been already pointed out in [5, 21, 37, 54] for the complex shifted preconditioner in two- and three-dimensional applications, when addressing problems of smaller dimension although. We note that the two-grid cycles used as a preconditioner usually require a moderate number of preconditioner applications (each application being however computationally expensive). As expected, using the combined cycles ($\mathcal{T}_{2,V}$, $\mathcal{T}_{3,V}$ or $\mathcal{T}_{3,F}$) leads to a significant decrease in terms of computational times with respect to the two-grid preconditioner ($\mathcal{T}$) initially proposed in [35]: a reduction factor of at least 1.5 is obtained even at high wavenumbers. This can be considered as a noticeable improvement. Furthermore we notice that the numbers of preconditioner applications obtained with the combined approaches are almost similar. Using a coarse preconditioner with a hierarchy of three grids such as in $\mathcal{T}_{3,V}$ or $\mathcal{T}_{3,F}$ allows us to reduce the computational

Table 3: Preconditioned flexible methods for the solution of the Helmholtz equation for the homogeneous velocity field. Case of a second-order discretization with 10 points per wavelength such that $kh = \pi/5$. Prec denotes the number of preconditioner applications, T the total computational time in seconds and M the requested memory in GB. Case of two-grid ($\mathcal{T}$), of complex shifted multigrid cycles ($\mathcal{M}_{4,V}$, $\mathcal{M}_{4,F}$) and of combined cycles ($\mathcal{T}_{2,V}$, $\mathcal{T}_{3,V}$ and $\mathcal{T}_{3,F}$) applied as a preconditioner of FGMRES(5). Numerical experiments performed on a IBM BG/P computer.

Homogeneous velocity field							
		$\mathcal{T}$			$\mathcal{T}_{2,V}$		
Grid	# Cores	Prec	T (s)	M (GB)	Prec	T (s)	M (GB)
128^3	1	18	455	0.3	17	309	0.3
256^3	8	29	790	2.4	28	552	2.4
512^3	64	49	1354	19.2	52	1047	19.5
1024^3	512	92	2588	154.0	100	2067	155.7
2048^3	4096	228	6593	1232.0	207	4447	1245.5
		$\mathcal{M}_{4,V}$			$\mathcal{M}_{4,F}$		
Grid	# Cores	Prec	T (s)	M (GB)	Prec	T (s)	M (GB)
128^3	1	95	251	0.3	125	372	0.3
256^3	8	180	505	2.0	180	573	2.0
512^3	64	355	1026	16.4	339	1107	16.4
1024^3	512	696	2112	130.8	635	2165	130.8
2048^3	4096	1415	4644	1046.8	1278	4634	1046.8
		$\mathcal{T}_{3,V}$			$\mathcal{T}_{3,F}$		
Grid	# Cores	Prec	T (s)	M (GB)	Prec	T (s)	M (GB)
128^3	1	17	**250**	0.3	18	289	0.3
256^3	8	29	**463**	2.4	30	528	2.4
512^3	64	54	**877**	19.6	56	1007	19.6
1024^3	512	105	**1746**	157.1	107	1980	157.1
2048^3	4096	259	**4442**	1256.5	247	4752	1256.5

times with respect to the $\mathcal{T}_{2,V}$ approach. Concerning the complex shifted preconditioners, we remark that the $\mathcal{M}_{4,V}$ strategy performs well in terms of computational times with respect to $\mathcal{M}_{4,F}$. Indeed on this homogeneous problem a preconditioner with a cycling strategy visiting only once the coarsest level such as the V-cycle seems to be a good compromise in terms of computational times. Among the six investigated preconditioning strategies, $\mathcal{T}_{3,V}$ always delivers the minimal computational times (see bold values in Table 3). Compared to $\mathcal{M}_{4,V}$, $\mathcal{T}_{3,V}$ leads to a reduction in terms of computational times of about 20% (1024^3) and of 4.5% on the largest test case (2048^3). Finally, we note that the maximal requested memory (M) grows linearly with the problem size whatever the preconditioner. This is indeed the expected behaviour since these strategies do not rely on any (local or global) factorization of sparse matrices. The complex shifted preconditioners $\mathcal{M}_{4,F}$ and $\mathcal{M}_{4,V}$ require less memory than the combined strategies $\mathcal{T}_{3,V}$ and $\mathcal{T}_{3,F}$: a factor of reduction of 20% is indeed observed. Furthermore we point out that the numerical methods investigated in this paper on both homogeneous or heterogeneous cases are relatively cheap in terms of memory requirements, e.g., an amount of only 157 GB at most is needed when solving a wave propagation problem with more than one billion of unknowns (1024^3). This feature is especially important when addressing in a near future the solution of multiple right-hand side problems arising in the related acoustic imaging inverse problem.

5.3 EAGE/SEG Salt dome

The SEG/EAGE Salt dome model [1] is a velocity field containing a salt dome in a sedimentary embankment. It is defined in a parallelepiped domain of size $13.5 \times 13.5 \times 4.2$ km^3. The minimum value of the velocity is 1500 $m.s^{-1}$ and its maximum value is 4481 $m.s^{-1}$, respectively. This test case is considered as challenging due to both the occurrence of a geometrically complex structure (salt dome) and to the large dimensions of the computational domain.

We are mostly interested in evaluating the behaviour of the different preconditioners versus the frequency on this heterogeneous velocity field problem. We consider a set of frequencies ranging from 2.5 Hz to 40 Hz with a step size h selected such that the stability condition (5) is satisfied. We note that the largest frequency case ($f = 40$ Hz) corresponds to a linear system of approximately 15.8 billion of unknowns. In the numerical experiments we analyse four different strategies: a two-grid preconditioner ($\mathcal{T}$), two three-grid complex shifted preconditioners ($\mathcal{M}_{3,V}$, $\mathcal{M}_{3,F}$) and a two-grid cycle with a two-grid complex shifted coarse preconditioner ($\mathcal{T}_{2,V}$), respectively. We have considered hierarchies with at most three grids to yield a reasonable problem size per core. As in Section 5.2, we have used relaxation parameters issued from the rigorous Fourier analysis (relation (16)).

Table 4: Preconditioned flexible methods for the solution of the Helmholtz equation for the heterogeneous velocity field EAGE/SEG Salt dome. Case of a second-order discretization with 10 points per wavelength such that relation (5) is satisfied. Prec denotes the number of preconditioner applications, T the total computational time in seconds and M the requested memory in GB. Case of two-grid ($\mathcal{T}$), of complex shifted multigrid cycles ($\mathcal{M}_{3,V}$, $\mathcal{M}_{3,F}$) and of combined cycles ($\mathcal{T}_{2,V}$) applied as a preconditioner of FGMRES(5). Numerical experiments performed on a IBM BG/P computer. A † superscript indicates that a maximal number of preconditioner applications has been reached.

EAGE/SEG Salt dome									
				$\mathcal{T}$			$\mathcal{T}_{2,V}$		
f	h	Grid	# Cores	Prec	T (s)	M (GB)	Prec	T (s)	M (GB)
2.5	60	$231 \times 231 \times 71$	4	12	146	0.6	11	**98**	0.6
5	30	$463 \times 463 \times 143$	32	25	316	4.5	16	**147**	4.6
10	15	$927 \times 927 \times 287$	256	71	927	35.9	28	**270**	36.6
20	7.5	$1855 \times 1855 \times 575$	2048	248	3346	288.1	73	**748**	293.8
40	3.75	$3711 \times 3711 \times 1149$	16384	$1000^{\dagger}$	13912	2304.1	283	**3101**	2349.9
				$\mathcal{M}_{3,V}$			$\mathcal{M}_{3,F}$		
f	h	Grid	# Cores	Prec	T (s)	M (GB)	Prec	T (s)	M (GB)
2.5	60	$231 \times 231 \times 71$	4	98	132	0.5	122	193	0.5
5	30	$463 \times 463 \times 143$	32	217	300	3.8	184	298	3.8
10	15	$927 \times 927 \times 287$	256	445	638	30.5	334	561	30.5
20	7.5	$1855 \times 1855 \times 575$	2048	2485	4102	244.8	2149	3764	244.8
40	3.75	$3711 \times 3711 \times 1149$	16384	$8000^{\dagger}$	-	1957.8	$8000^{\dagger}$	-	1957.8

Table 4 collects the number of preconditioner applications (Prec), computational times (T) and maximal requested memory (M) for these variants. With respect to the two-grid cycle $\mathcal{T}$, the combined cycle $\mathcal{T}_{2,V}$ is found to require a reduced number of preconditioner applications. Indeed, if we consider the case of $f = 20$ Hz, we remark a significant reduction of preconditioner applications when comparing the two-grid preconditioner $\mathcal{T}$ with the combined two-grid cycle $\mathcal{T}_{2,V}$ (248 versus 73). This also leads to a dramatic reduction of computational times (3346 s versus 748 s at $f = 20$ Hz). The $\mathcal{T}_{2,V}$ strategy always delivers the minimal computational times (see bold values in Table 4) among the four preconditioners with a clear advantage at medium to large frequencies. Nevertheless we would like to stress that the shifted preconditioner presented in Algorithm 2 is based on a combination of standard multigrid components. It is most likely that the use of Galerkin coarse grid approximation or of operator-dependent transfer operators could be beneficial to improve the properties of the preconditioner when considering heterogeneous Helmholtz problems. Despite the simplicity of the shifted preconditioner we remark that both $\mathcal{M}_{3,V}$ and $\mathcal{M}_{3,F}$ strategies are more attractive than

the two-grid preconditioner $\mathcal{T}$ in terms of computational times at small to medium range frequencies (2.5 Hz, 5 Hz and 10 Hz respectively). However at high frequencies (20 Hz and 40 Hz) a significant increase in terms of preconditioning applications is observed for both $\mathcal{M}_{3,V}$ and $\mathcal{M}_{3,F}$. We also notice that a shifted preconditioner based on a F-cycle is preferable when large frequencies are considered, i.e. solving approximately the coarse problem twice in a given cycle is found to be beneficial to the outer convergence.

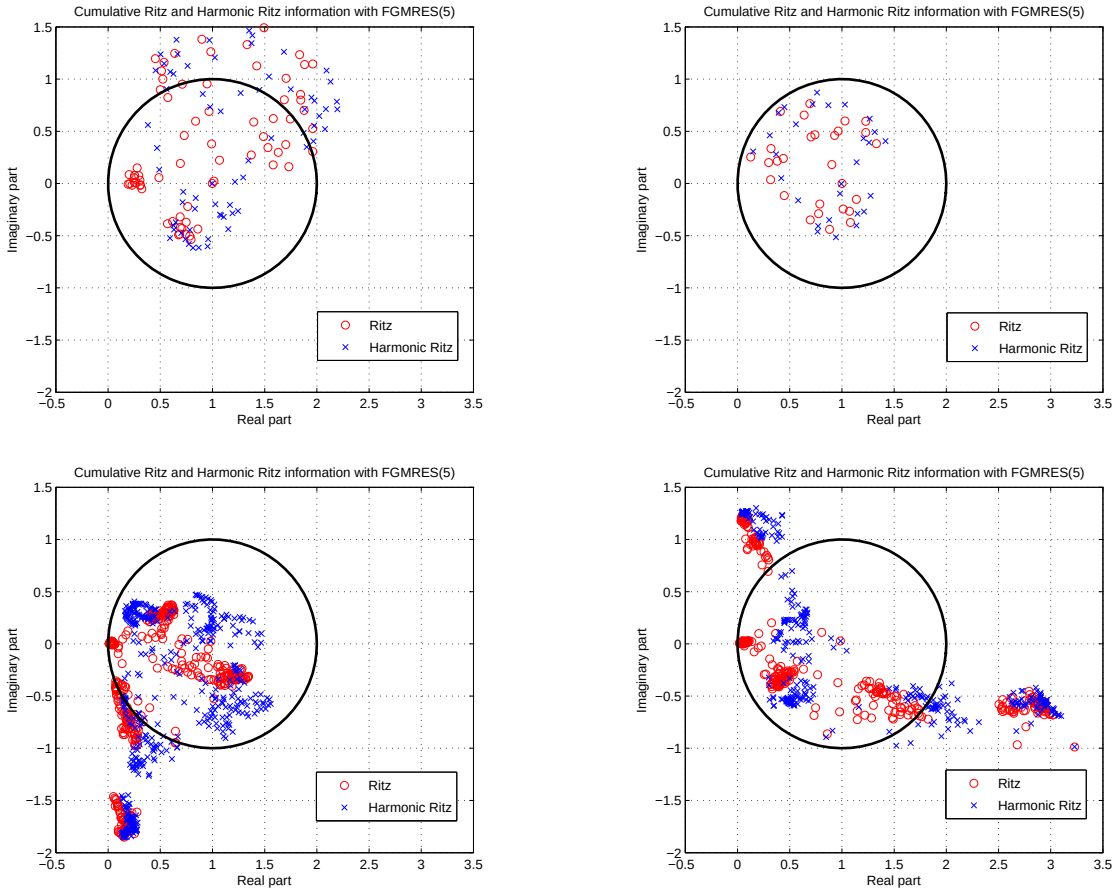

Figure 7: EAGE/SEG Salt dome problem (case of $f = 10$ Hz, $927 \times 927 \times 287$ grid). Ritz and harmonic Ritz values (circles and crosses, respectively) of FGMRES(5) with four different variable preconditioners: $\mathcal{T}$ (top left), $\mathcal{T}_{2,V}$ (top right), $\mathcal{M}_{3,V}$ (bottom left) and $\mathcal{M}_{3,F}$ (bottom right) along convergence. Note that the same scales have been used for the four plots.

In Figure 7 we consider the case of $f = 10$ Hz and represent the Ritz and harmonic Ritz values collected at each cycle of FGMRES(5) during convergence. As shown in [35], this computation allows us to investigate the quality of the *variable* preconditioner

at a cheap cost and we refer the reader to [26] for the definition of Ritz and harmonic Ritz values in this setting. Interestingly, the $\mathcal{T}$, $\mathcal{M}_{3,V}$ and $\mathcal{M}_{3,F}$ preconditioners lead to several outliers or clusters located in specific parts of the complex plane (even in the vicinity of the origin), whereas all Ritz or harmonic Ritz values are located in the unit disk (reasonably away from the origin) for the $\mathcal{T}_{2,V}$ preconditioner. Finally, we note that the combined cycle $\mathcal{T}_{2,V}$ used as a preconditioner of FGMRES(5) is also efficient when solving the largest frequency case ($f = 40$ Hz). A moderate number of preconditioner applications (283) and a low memory requirement (about 2.3 TB) are required to solve approximately this truly challenging case. This can be considered as a very satisfactory result and proves the usefulness of the algorithm on this realistic test case.

Remarks We have also performed some numerical experiments with a larger value of the restarting parameter m in the outer Krylov subspace method FGMRES(m) ($m = 10$, results not shown here). At $f = 20$ Hz, a reduction of preconditioner applications is obtained for each strategy leading to a decrease of 10% in computational times. This slight improvement comes however at a price of increased memory requirements. Keeping memory consumption as low as possible is an important issue in this application since we target the solution of multiple right-hand side problems with preconditioned block flexible Krylov subspace methods as discussed in [9]. Hence we have preferred to focus on preconditioned FGMRES(5) in this section and to show the related performance even for such moderate value of the restarting parameter m. We refer the reader to [43] for a theoretical analysis of inner-outer methods when the outer and the inner methods are the same (FGMRES and GMRES in our setting). It is notably proved that by using preconditioners which are Krylov methods the global iteration is maintained within a larger Krylov subspace.

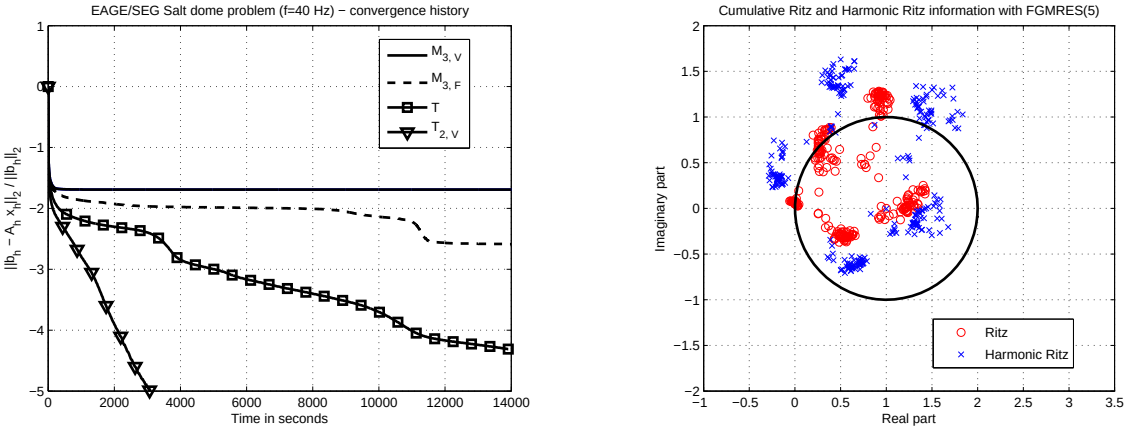

Figure 8: EAGE/SEG Salt dome problem (case of $f = 40$ Hz, $3711 \times 3711 \times 1149$ grid). Convergence history of FGMRES(5) with four different variable preconditioners: $\mathcal{M}_{3,V}$ (line), $\mathcal{M}_{3,F}$ (dashed line), $\mathcal{T}$ (square) and $\mathcal{T}_{2,V}$ (triangle) versus computational times in seconds (left part). Ritz and harmonic Ritz values (circles and crosses, respectively) of FGMRES(5) with the $\mathcal{T}_{2,V}$ preconditioner (right part).

Figure 8 (left part) shows the convergence history of FGMRES(5) with four different preconditioners, namely $\mathcal{T}$, $\mathcal{M}_{3,V}$, $\mathcal{M}_{3,F}$, and $\mathcal{T}_{2,V}$ on the most challenging case ($f = 40$ Hz, approximately 15.8 billion of unknowns). Interestingly, we notice that the stopping criterion (27) is satisfied only for FGMRES(5) used in combination with the new preconditioner $\mathcal{T}_{2,V}$ (see right part of Figure 8 for the repartition of Ritz and harmonic Ritz values). The $\mathcal{T}$, $\mathcal{M}_{3,V}$ and $\mathcal{M}_{3,F}$ approaches lead to a certain residual reduction but due to limited computing resources we have only reported the maximal number of preconditioner applications and related elapsed computational times in Table 4. We remark that a long-term stagnation in the convergence does appear for the shifted preconditioner. We further plan to analyse this behaviour in the light of recent non-stagnation conditions for the convergence of GMRES on indefinite problems [42, 45] as part of future work. Contrary to the case of $f = 20$ Hz (Figure 7, top right part) Ritz and harmonic Ritz with negative real part are observed at $f = 40$ Hz (Figure 8, right part) for the $\mathcal{T}_{2,V}$ combined preconditioner[3]. We refer the reader to comments given in the last paragraph of this section for possible improvements related to both preconditioner and outer Krylov subspace method.

[3]More precisely 25 Ritz values with negative real part (smallest modulus equal to 0.05) and 56 harmonic Ritz values with negative real part (smallest modulus equal to 0.29) are obtained.

Table 5: Preconditioned flexible methods for the solution of the Helmholtz equation for the heterogeneous velocity field EAGE/SEG Salt dome. Case of a second-order discretization with 10 points per wavelength such that relation (5) is satisfied. Prec denotes the number of preconditioner applications, T the total computational time in seconds and M the requested memory in GB. Case of two-grid cycles applied as a preconditioner of FGMRES(5). Numerical experiments performed on a IBM BG/P computer. Influence of the fine level smoother.

EAGE/SEG Salt dome								
			$\mathcal{T}$ $(\vartheta = 2, m_s = 2, \nu = 0)$			$\mathcal{T}$ $(\vartheta = 1, m_s = 4, \nu = 0)$		
f	Grid	# Cores	Prec	T (s)	M (GB)	Prec	T (s)	M (GB)
2.5	$231 \times 231 \times 71$	4	11	77	0.6	11	76	0.6
5	$463 \times 463 \times 143$	32	24	174	4.5	24	172	4.9
10	$927 \times 927 \times 287$	256	54	409	35.9	54	402	39.8
20	$1855 \times 1855 \times 575$	2048	180	1420	288.1	178	1381	319.5
40	$3711 \times 3711 \times 1149$	16384	1343	11180	2304.1	1244	10169	2444.7
			$\mathcal{T}_{2,V}$ $(\vartheta = 2, m_s = 2, \nu = 0)$			$\mathcal{T}_{2,V}$ $(\vartheta = 1, m_s = 4, \nu = 0)$		
f	Grid	# Cores	Prec	T (s)	M (GB)	Prec	T (s)	M (GB)
2.5	$231 \times 231 \times 71$	4	11	89	0.6	11	88	0.9
5	$463 \times 463 \times 143$	32	16	135	4.6	16	133	6.0
10	$927 \times 927 \times 287$	256	28	247	36.6	27	235	43.0
20	$1855 \times 1855 \times 575$	2048	72	683	293.8	72	672	325.2
40	$3711 \times 3711 \times 1149$	16384	313	3929	2349.9	313	3885	2522.1

We report numerical results in Table 5 related to the $\mathcal{T}$ and $\mathcal{T}_{2,V}$ cycles, now with a different smoothing strategy at the fine level only. A fine level smoother based on either one cycle of unpreconditioned GMRES(4) ($\vartheta = 1$, $m_s = 4$ and $\nu = 0$) or two cycles of unpreconditioned GMRES(2) ($\vartheta = 2$, $m_s = 2$ and $\nu = 0$) is investigated (without any changes for the other parameters). This choice leads to the same number of matrix-vector products to be performed in the smoother on the fine level as the initial setting ($\vartheta = 1$, $m_s = 2$ and $\nu = 2$). Interestingly we note a significant reduction in terms of preconditioner applications for medium to large frequencies for the two-grid preconditioner $\mathcal{T}$. For this approach performing more smoothing iterations by either restarting or increasing the degree of the polynomial smoother is then found to be beneficial on this given application. For the combined cycle $\mathcal{T}_{2,V}$ the change of the fine level smoother does not modify the number of preconditioner applications and leads to a reduction of at least 10% in terms of computational times for frequencies up to 20 Hz (see Table 4 for a comparison). At $f = 40$ Hz the cycle with preconditioned GMRES(2) ($\vartheta = 1$, $m_s = 2$ and $\nu = 2$) leads to better results in terms of preconditioner applications and computational times. Finally we note that optimizing the sparse matrix-vector products [13] and considering communication avoiding GMRES method [30] in both the inner and

outer Krylov subspace methods are two features that would be worth investigating to further reduce the computational times.

We have on purpose restricted our setting to simple multigrid components to be able to perform a rigorous Fourier analysis. Nevertheless we are aware of possible improvements in the proposed algorithms. Indeed smoothers based on symmetric Gauss-Seidel preconditioned GMRES (as studied in [35]), the use of Galerkin coarse grid approximation or of complex-valued operator-dependent transfer operators [54] might be probably beneficial to the preconditioners on heterogeneous problems. Moreover, given a certain preconditioner, considering the role of the flexible Krylov subspace method is certainly an issue to address in a near future. Other flexible methods [49, 60] or recent algorithms that include spectral information to improve the convergence rate - FGMRES-DR [26] or FGCRO-DR [10] - are definitively of interest in both inner and outer parts of the solver.

6 Conclusions

We have proposed a new two-grid preconditioner for the solution of Helmholtz problems in three-dimensional heterogeneous media. This two-grid cycle is applied directly to the Helmholtz operator and relies on an approximate coarse grid solution. A second multigrid method applied to a complex shifted Laplacian operator is then used as a preconditioner for the approximate solution of this coarse problem. Next, we have studied the convergence properties of this preconditioner with rigorous Fourier analysis and selected appropriate relaxation parameters for the smoother based on this analysis. Finally we have highlighted the efficiency of the new preconditioner on both academic and concrete applications in geophysics requiring the solution of indefinite problems of huge dimension. Numerical results have demonstrated the usefulness of the combined algorithm on a realistic three-dimensional application at high frequency.

As part of future research, we plan to perform a three-grid Fourier analysis of the combined cycle to yield additional valuable insight into the preconditioning properties of this method. We will also investigate the behaviour of the combined preconditioner on problems issued from the high-order finite difference discretization of the acoustic or elastic Helmholtz equation [29] in both single and multiple source situations. To conclude, we note that the framework of the combined cycle can be extended to a fully algebraic setting by using algebraic multigrid ideas [53, Appendix A] (see also [32] for a specific extension to complex-valued problems) to construct the different operators involved in the two hierarchies. This may be especially useful when finite element discretizations of the Helmholtz equation (based, e.g., on Discontinuous Galerkin methods or on *hp*-finite element techniques) are considered. This is part of future research.

Acknowledgments

The authors would like to thank the two referees for their valuable comments and suggestions that helped us to improve the manuscript. They thank Prof. A. Borzi and Prof. C. W. Oosterlee for the invitation to the OPTPDE ESFWaves workshop held in Würzburg, Germany on September 26-28th 2011. They also would like to acknowledge GENCI (Grand Equipement National de Calcul Intensif) for the dotation of computing hours on the IBM BG/P computer at IDRIS, France. This work was granted access to the HPC resources of CINES and IDRIS under allocation 2011065068 and 2012065068 made by GENCI.

References

[1] F. Aminzadeh, J. Brac, and T. Kunz. 3D Salt and Overthrust models. SEG/EAGE modeling series I, Society of Exploration Geophysicists, 1997. 26

[2] A. Bayliss, C. I. Goldstein, and E. Turkel. An iterative method for the Helmholtz equation. *J. Comp. Phys.*, 49:443–457, 1983. 2

[3] J.-P. Berenger. A perfectly matched layer for absorption of electromagnetic waves. *J. Comp. Phys.*, 114:185–200, 1994. 4

[4] J.-P. Berenger. Three-dimensional perfectly matched layer for absorption of electromagnetic waves. *J. Comp. Phys.*, 127:363–379, 1996. 4, 5

[5] M. Bollhöfer, M. J. Grote, and O. Schenk. Algebraic multilevel preconditioner for the solution of the Helmholtz equation in heterogeneous media. *SIAM J. Scientific Computing*, 31:3781–3805, 2009. 2, 6, 8, 24

[6] A. Brandt and I. Livshits. Wave-ray multigrid method for standing wave equations. *Electronic Transactions on Numerical Analysis*, 6:162–181, 1997. 2

[7] A. Brandt and S. Ta'asan. Multigrid method for nearly singular and slightly indefinite problems. In W. Hackbusch and U. Trottenberg, editors, *Multigrid Methods II*, pages 99–121. Springer, 1986. 2

[8] H. Calandra, S. Gratton, R. Lago, X. Pinel, and X. Vasseur. Two-level preconditioned Krylov subspace methods for the solution of three-dimensional heterogeneous Helmholtz problems in seismics. *Numerical Analysis and Applications*, 5:175–181, 2012. 3

[9] H. Calandra, S. Gratton, J. Langou, X. Pinel, and X. Vasseur. Flexible variants of block restarted GMRES methods with application to geophysics. *SIAM J. Sci. Comput.*, 34(2):A714–A736, 2012. 3, 24, 29

[10] L.M. Carvalho, S. Gratton, R. Lago, and X. Vasseur. A flexible generalized conjugate residual method with inner orthogonalization and deflated restarting. *SIAM J. Matrix Analysis and Applications*, 32(4):1212–1235, 2011. 32

[11] G. Cohen. *Higher-order numerical methods for transient wave equations*. Springer, 2002. 5

[12] S. Cools and W. Vanroose. Local Fourier analysis of the complex shifted Laplacian preconditioner for Helmholtz problems. Technical report, University of Antwerp, Department of Mathematics and Computer Science, Belgium, 2011. 15

[13] K. Datta, S. Kamil, S. Williams, L. Oliker, J. Shalf, and K. Yelick. Optimization and performance modeling of stencil computations on modern microprocessors. *SIAM Review*, 51(1):129–159, 2009. 31

[14] I. S. Duff, S. Gratton, X. Pinel, and X. Vasseur. Multigrid based preconditioners for the numerical solution of two-dimensional heterogeneous problems in geophysics. *International Journal of Computer Mathematics*, 84-88:1167–1181, 2007. 17

[15] H. Elman, O. Ernst, D. O'Leary, and M. Stewart. Efficient iterative algorithms for the stochastic finite element method with application to acoustic scattering. *Comput. Methods Appl. Mech. Engrg.*, 194(1):1037–1055, 2005. 3, 6

[16] H. C. Elman, O. G. Ernst, and D. P. O'Leary. A multigrid method enhanced by Krylov subspace iteration for discrete Helmholtz equations. *SIAM J. Scientific Computing*, 23:1291–1315, 2001. 3, 6, 7, 13, 21

[17] B. Engquist and L. Ying. Sweeping preconditioner for the Helmholtz equation: moving perfectly matched layers. *Multiscale Modeling and Simulation*, 9:686–710, 2011. 6, 8

[18] Y. A. Erlangga. *A robust and efficient iterative method for the numerical solution of the Helmholtz equation*. PhD thesis, TU Delft, 2005. 2

[19] Y. A. Erlangga. Advances in iterative methods and preconditioners for the Helmholtz equation. *Archives of Computational Methods in Engineering*, 15:37–66, 2008. 2, 8

[20] Y. A. Erlangga and R. Nabben. On a multilevel Krylov method for the Helmholtz equation preconditioned by shifted Laplacian. *Electronic Transactions on Numerical Analysis*, 31:403–424, 2008. 3, 6

[21] Y. A. Erlangga, C. Oosterlee, and C. Vuik. A novel multigrid based preconditioner for heterogeneous Helmholtz problems. *SIAM J. Scientific Computing*, 27:1471–1492, 2006. 2, 6, 7, 8, 12, 13, 15, 17, 24

[22] Y. A. Erlangga, C. Vuik, and C. Oosterlee. On a class of preconditioners for solving the Helmholtz equation. *Appl. Num. Math.*, 50:409–425, 2004. 2, 7

[23] O. Ernst and M. J. Gander. Why it is difficult to solve Helmholtz problems with classical iterative methods. In O. Lakkis I. Graham, T. Hou and R. Scheichl, editors, *Numerical Analysis of Multiscale Problems*. Springer, 2011. 2, 6

[24] C. Farhat, A. Macedo, and M. Lesoinne. A two-level domain decomposition method for the iterative solution of high frequency exterior Helmholtz problems. *Numerische Mathematik*, 85:283–308, 2000. 2

[25] C. Farhat and F. X. Roux. A method of finite element tearing and interconnecting and its parallel solution algorithm. *Internat. J. Numer. Meths. Engrg.*, 32:1205–1227, 1991. 2

[26] L. Giraud, S. Gratton, X. Pinel, and X. Vasseur. Flexible GMRES with deflated restarting. *SIAM J. Scientific Computing*, 32:1858–1878, 2010. 29, 32

[27] W. Gropp, E. Lusk, and A. Skjellum. *Using MPI: Portable Parallel Programming with the Message-Passing Interface*. MIT Press, 1999. 24

[28] W. Hackbusch and U. Trottenberg. *Multigrid methods*. Springer, 1982. Lecture Notes in Mathematics, vol. 960, Proceedings of the conference held at Köln-Porz, November 23-27 1981. 19

[29] I. Harari and E. Turkel. Accurate finite difference methods for time-harmonic wave propagation. *J. Comp. Phys.*, 119:252–270, 1995. 32

[30] M. Hoemmen. *Communication-avoiding Krylov subspace methods*. PhD thesis, University of California, Berkeley, Department of Computer Science, 2010. 31

[31] A. L. Laird and M. B. Giles. Preconditioned iterative solution of the 2D Helmholtz equation. Technical Report Report NA-02/12, Oxford University Computing Laboratory, 2002. 2

[32] S. P. MacLachlan and C. W. Oosterlee. Algebraic multigrid solvers for complex-valued matrices. *SIAM J. Scientific Computing*, 30:1548–1571, 2008. 32

[33] Y. Notay and P. S. Vassilevski. Recursive Krylov-based multigrid cycles. *Numerical Linear Algebra with Applications*, 15:473–487, 2008. 9

[34] S. Operto, J. Virieux, P. R. Amestoy, J.-Y. L'Excellent, L. Giraud, and H. Ben Hadj Ali. 3D finite-difference frequency-domain modeling of visco-acoustic wave propagation using a massively parallel direct solver: A feasibility study. *Geophysics*, 72-5:195–211, 2007. 5, 21

[35] X. Pinel. *A perturbed two-level preconditioner for the solution of three-dimensional heterogeneous Helmholtz problems with applications to geophysics*. PhD thesis, CERFACS, 2010. TH/PA/10/55, available at http://www.cerfacs.fr/algor/reports/Dissertations/TH_PA_10_55.pdf. 3, 5, 6, 7, 16, 24, 28, 32

[36] B. Reps, W. Vanroose, and H. bin Zubair. On the indefinite Helmholtz equation: complex stretched absorbing boundary layers, iterative analysis, and preconditioning. *J. Comp. Phys.*, 229:8384–8405, 2010. 6

[37] C. D. Riyanti, A. Kononov, Y. A. Erlangga, R.-E. Plessix, W. A. Mulder, C. Vuik, and C. Oosterlee. A parallel multigrid-based preconditioner for the 3D heterogeneous high-frequency Helmholtz equation. *J. Comp. Phys.*, 224:431–448, 2007. 2, 3, 8, 24

[38] Y. Saad. A flexible inner-outer preconditioned GMRES algorithm. *SIAM J. Scientific and Statistical Computing*, 14:461–469, 1993. 9

[39] Y. Saad. *Iterative Methods for Sparse Linear Systems.* SIAM, Philadelphia, 2003. Second edition. 19

[40] Y. Saad and M. H. Schultz. GMRES: A generalized minimal residual algorithm for solving nonsymmetric linear systems. *SIAM J. Scientific and Statistical Computing*, 7:856–869, 1986. 6

[41] A.H. Sheikh, D. Lahaye, and C. Vuik. A scalable Hemholtz solver combining the shifted Laplace preconditioner with multigrid deflation. Report 11-01, Delft University of Technology, Delft Institute of Applied Mathematics, Delft, 2011. 3

[42] V. Simoncini. On a non-stagnation condition for GMRES and application to saddle point matrices. *Electronic Transactions on Numerical Analysis*, 37:202–213, 2010. 30

[43] V. Simoncini and D. B. Szyld. Flexible inner-outer Krylov subspace methods. *SIAM J. Numerical Analysis*, 40:2219–2239, 2003. 9, 29

[44] V. Simoncini and D. B. Szyld. Recent computational developments in Krylov subspace methods for linear systems. *Numerical Linear Algebra with Applications*, 14:1–59, 2007. 9

[45] V. Simoncini and D. B. Szyld. New conditions for non-stagnation of minimal residual methods. *Numerische Mathematik*, 109:477–487, 2008. 30

[46] F. Sourbier, S. Operto, J. Virieux, P. Amestoy, and J. Y. L' Excellent. FWT2D : a massively parallel program for frequency-domain full-waveform tomography of wide-aperture seismic data - part 1: algorithm. *Computer & Geosciences*, 35:487–495, 2009. 5

[47] F. Sourbier, S. Operto, J. Virieux, P. Amestoy, and J. Y. L' Excellent. FWT2D : a massively parallel program for frequency-domain full-waveform tomography of wide-aperture seismic data - part 2: numerical examples and scalability analysis. *Computer & Geosciences*, 35:496–514, 2009. 5

[48] K. Stüben and U. Trottenberg. Multigrid methods: fundamental algorithms, model problem analysis and applications. In W. Hackbusch and U. Trottenberg, editors, *Multigrid methods, Koeln-Porz, 1981, Lecture Notes in Mathematics, volume 960.* Springer, 1982. 3, 6, 8, 10, 13

[49] D. B. Szyld and J. A. Vogel. FQMR: A flexible quasi-minimal residual method with inexact preconditioning. *SIAM J. Scientific Computing*, 23(2):363–380, 2001. 32

[50] A. Tarantola. *Inverse problem theory and methods for model parameter estimation.* SIAM, 2005. 4

[51] C. A. Thole and U. Trottenberg. Basic smoothing procedures for the multigrid treatment of elliptic 3D operators. *Appl. Math. Comput.*, 19:333–345, 1986. 10

[52] A. Toselli and O. Widlund. *Domain Decomposition methods - Algorithms and Theory.* Springer Series on Computational Mathematics, Springer, 34, 2005. 2

[53] U. Trottenberg, C. W. Oosterlee, and A. Schüller. *Multigrid.* Academic Press Inc., 2001. 6, 10, 11, 13, 16, 19, 24, 32

[54] N. Umetani, S. P. MacLachlan, and C. W. Oosterlee. A multigrid-based shifted Laplacian preconditioner for fourth-order Helmholtz discretization. *Numerical Linear Algebra with Applications*, 16:603–626, 2009. 24, 32

[55] M. B. van Gijzen, Y. A. Erlangga, and C. Vuik. Spectral analysis of the discrete Helmholtz operator preconditioned with a shifted Laplacian. *SIAM J. Scientific Computing*, 29:1942–1958, 2007. 2, 3, 8

[56] W. Vanroose, B. Reps, and H. bin Zubair. A polynomial multigrid smoother for the iterative solution of the heterogeneous Helmholtz problem. Technical Report, University of Antwerp, Belgium, 2010. http://arxiv.org/abs/1012.5379. 6

[57] P. S. Vassilevski. *Multilevel Block Factorization Preconditioners, Matrix-based Analysis and Algorithms for Solving Finite Element Equations.* Springer, New York, 2008. 9

[58] J. Virieux and S. Operto. An overview of full waveform inversion in exploration geophysics. *Geophysics*, 74(6):WCC127–WCC152, 2009. 4

[59] J. Virieux, S. Operto, H. Ben Hadj Ali, R. Brossier, V. Etienne, F. Sourbier, L. Giraud, and A. Haidar. Seismic wave modeling for seismic imaging. *The Leading Edge*, 25(8):538–544, 2009. 6, 8

[60] J. A. Vogel. Flexible BiCG and flexible Bi-CGSTAB for nonsymmetric linear systems. *Appl. Math. Comput.*, 188:226–233, 2007. 32

[61] S. Wang, M. V. de Hoop, and J. Xia. Acoustic inverse scattering via Helmholtz operator factorization and optimization. *J. Comp. Phys.*, 229:8445–8462, 2010. 5

[62] S. Wang, M. V. de Hoop, and J. Xia. On 3D modeling of seismic wave propagation via a structured parallel multifrontal direct Helmholtz solver. *Geophysical Prospecting*, 59:857–873, 2011. 5

[63] R. Wienands, C. W. Oosterlee, and T. Washio. Fourier analysis of GMRES(m) preconditioned by multigrid. *SIAM J. Scientific Computing*, 22:582–603, 2000. 13, 15, 17

[64] P. M. De Zeeuw. Matrix-dependent prolongations and restrictions in a blackbox multigrid solver. *J. Comput. Appl. Math.*, 33:1–27, 1990. 8